NASA Technical Memorandum

NASA TM -86573

THE EFFECTS OF GRAVITY LEVEL DURING DIRECTIONAL SOLIDIFICATION ON THE MICROSTRUCTURE OF HYPERMONOTECTIC Al-In-Sn ALLOYS

Center Director's Discretionary Fund Final Report

By P. A. Curreri and W. F. Kaukler

Space Science Laboratory
Science and Engineering Directorate

November 1986

National Aeronautics and Space Administration

George C. Marshall Space Flight Center

TECHNICAL REPORT STANDARD TITLE PAGE

1. REPORT NO.	2. GOVERNMENT ACCESSION NO.	3. RECIPIENT'S CATALOG NO.
NASA TM-86573		

4. TITLE AND SUBTITLE

The Effects of Gravity Level During Directional Solidification on the Microstructure of Hypermonotectic Al-In-Sn Alloys

5. REPORT DATE November 1986

6. PERFORMING ORGANIZATION CODE

7. AUTHOR(S)

P. A. Curreri and W. F, Kaukler*

8. PERFORMING ORGANIZATION REPORT #

9. PERFORMING ORGANIZATION NAME AND ADDRESS

George C. Marshall Space Flight Center
Marshall Space Flight Center, Alabama 35812

10. WORK UNIT NO.

11. CONTRACT OR GRANT NO.

12. SPONSORING AGENCY NAME AND ADDRESS

National Aeronautics and Space Administration
Washington, D.C. 20546

13. TYPE OF REPORT & PERIOD COVERED

Technical Memorandum

14. SPONSORING AGENCY CODE

15. SUPPLEMENTARY NOTES

Prepared by Space Science Laboratory, Science and Engineering Directorate.

*Department of Chemistry, University of Alabama in Huntsville, Huntsville, AL 35899.

16. ABSTRACT

Five hypermonotectic Al-In-Sn compositions were directionally solidified in a Bridgman-type furnace at normal gravity and during aircraft low-gravity maneuvers. The tendency of the Al-30In alloy to form an indium-rich band at the start of unidirectional growth (SUG) made it difficult to study the integration of L_2 into the solidification interface. Hypermonotectic compositions closer to monotectic "slightly hypermonotectic" caused only a partial band of L_2 to form at SUG and allowed the study of such variables as gravity, composition, and monotectic dome height on integration of excess L_2 into the solid plus L_2 interface. It was found that formation of aligned composite structures for the Al-In-Sn system is not only a function of G and R but also of the degree to which the composition varies from on monotectic. Most of the aligned fibrous structures formed from hypermonotectic Al-In-Sn had spacings that were of the order of irregular fibrous structures reported for on monotectic Al-In-Sn. The spacings for the large fibers and aligned globules found for ground and low-gravity processed Al-18In-22Sn, respectively, were significantly larger than the others measured and were of the order expected for cell spacings under the growth conditions utilized. It was found that the integration into the solidification front of excess L_2 in low gravity was a function of the Sn composition of the alloy.

17. KEY WORDS	18. DISTRIBUTION STATEMENT
Low-Gravity Alloy Solidification, Immiscible Alloys, Al-In-Sn, Hypermonotectic, Directional Solidification During KC-135 Low-Gravity Maneuvers	Unclassified – Unlimited

19. SECURITY CLASSIF. (of this report)	20. SECURITY CLASSIF. (of this page)	21. NO. OF PAGES	22. PRICE
Unclassified	Unclassified	40	NTIS

MSFC - Form 3292 (May 1969)

For sale by National Technical Information Service, Springfield, Virginia 22151

ACKNOWLEDGMENTS

The authors wish to thank M. H. McCay whose encouragement and enthusiasm were instrumental to beginning this work. We wish to acknowledge the assistance of D. Warden for preparative and photometallography, W. K. Witherow for image analysis, and R. E. Shurney, G. Smith, R. Bond, J. Theiss, and G. Workman for providing the technical expertise needed to integrate and operate the directional solidification furnace in the KC-135 aircraft flight environment. We wish to also thank the Johnson Space Center personnel who operate the KC-135 aircraft. This research was supported by the Marshall Space Flight Center Director's Discretionary Fund and the NASA Microgravity Science and Applications Program.

TABLE OF CONTENTS

LIST OF ILLUSTRATIONS

LIST OF ILLUSTRATIONS (Concluded)

TECHNICAL MEMORANDUM

THE EFFECTS OF GRAVITY LEVEL DURING DIRECTIONAL SOLIDIFICATION ON THE MICROSTRUCTURE OF HYPERMONOTECTIC Al-In-Sn ALLOYS

I. INTRODUCTION

Many potentially important alloy systems have a monotectic dome (a region in their phase diagram where two immiscible liquid phases simultaneously exist). During solidification through the monotectic dome the alloy is especially susceptible to buoyancy-driven segregation. For this reason the low gravity of space is particularly attractive for the study of the solidification mechanisms of monotectic alloys, and for the processing of monotectic alloys with microstructures and properties that are not possible in the presence of gravitationally-driven segregation. This paper reports on results of experiments on directional solidification of immiscible Al-In-Sn alloys during aircraft multiple low-gravity maneuvers.

Like eutectic alloys, monotectic alloys can be made to grow with both regular and irregular aligned composite structures depending on growth rate, R, thermal gradient, G, and composition [1,2]. For monotectic alloys the interfacial energies between the two liquid phases (L_1 and L_2) and the wetting of the liquid phases to the solid (S_1) are believed to play a critical role in determining the solidified microstructure [3]. If L_2 west S_1 steady state growth and regular composite structures can be obtained if G/R is sufficiently large. However, since L_1 is chemically closer to S_1 it is likely that L_1 will be the wetting liquid in most monotectics. Theory predicts [3] that even if L_2 is not the wetting phase, composite growth can occur if the growth velocity is large enough to overcome the disjoining pressure. Further, it is expected that L_1 will perfectly wet S_1 unless the monotectic temperature is far below the critical temperature. To test these theories it was suggested that ternary monotectic systems be studied where the third component would change the monotectic dome height and provide a range disjoining pressures. Experimental studies of the solidification of Al-In-Sn [4,5] and the Al-Cu-Pb [4,5] have verified that as the concentration of the third component increases, lowering the monotectic dome height, there is a transition from steady state composite-type growth to irregular composite-type growth.

The influence of gravity on monotectic solidification has been studied to a limited extent by furnace inversion techniques. By changing the orientation of the solidification direction relative to the gravitational vector, the relative sensitivity of the monotectic microstructure to the presence of gravity can be determined [5,7,8]. Furnace inversion has limited use for studying hypermonotectic compositions, since the magnitude of the gravitational field remains constant and only the direction of the segregation relative to the solidification interface is changed [9].

Experimentation under the reduced gravity conditions of free fall or in space offers an opportunity to study hypermonotectic alloy solidification free from buoyancy-driven segregation. Solidification of hypermonotectic alloys in low gravity has sometimes resulted in greatly reduced macrosegregation [10-13], but has more often resulted in massive segregation caused by other nonbuoyancy-driven mechanisms [14-18] that normally would have been masked by the effect of gravity. These results clearly show the need for the detailed systematic investigations that can separate buoyancy-driven segregation from other mechanisms such as surface tension-driven flows and particle pushing by the solidification interface. In this study hypermonotectic Al-In-Sn

alloys over a composition range in which the solidification mechanism normally ranges from steady state composite for the lower Sn compositions to irregular composite growth for the higher Sn compositions are directionally solidified under normal gravity and during KC-135 low-gravity maneuvers.

II. EXPERIMENTAL METHOD

A. Directional Solidification Furnace System

The directional soldification furnace utilized in this research is the same unit that has been used in previously described studies on superalloys [19,20] and iron-carbon alloys [21,22]. The furnace is of the Bridgman type, equipped with a platinum rhodium resistance heating wire double wound around an alumina core below which is a water-cooled copper quench block. A sample of about 8 cm in length and 0.4 cm in diameter was placed in an alumina crucible 0.5 cm id and 45 cm long, with argon passing through the top. The furnace was positioned such that the bottom 1.5 to 2.0 cm of the sample remained unmelted. After about 10 min at temperature, the furnace was then translated upwards at controlled rates, the remainder of the sample being thus solidified.

The thermal profile of the furnace was such that the maximum temperature was 1040°C and about a 6 cm length of the crucible interior was above 900°C. The thermal gradient was determined with samples instrumented with an alumina coated thermocouple. The thermal gradient calculated at 640°C was 219°C/cm. The thermal gradients measured in this manner were found to be reproducible within 10 percent. Within this experimental error the gradients for flight and ground-based samples were found to remain consistent for solidification under all the gravitational conditions studied.

B. KC-135 Aircraft Furnace Integration

The method used in this research for studying the effects of low-g on solidification was to have the directional furnace flown on the NASA KC-135 aircraft during repetitive low-g maneuvers. Each maneuver gives from 20 to 30 sec of low-g (10^{-2} g, where g is 980 cm/sec^2), and up to 1.5 min of pullout and climb (up to 1.8 g). Therefore, a sample that is being solidified experiences a repetitive sequence of low-gravity (low-g) and high-gravity (high-g) forces parallel to the longitudinal growth axis. Acceleration experienced by the sample is monitored by three accelerometers mounted to the furnace assembly on three orthogonal axes. For a typical maneuver during low-g, the acceleration on all axes averages below 10^{-2} g. During pullout and climb, the high-g acceleration parallel to the longitudinal axis of the sample reaches 1.75 g, while the accelerations on the other two axes are less than 0.15 g.

The furnace translation rate is kept constant regardless of power fluctuations by a servo control circuit which maintains constant drive r/min. The furnace translation rate during each experiment is measured directly by a calibrated potentiometric translation detector and continuously recorded. The rate for these experiments was maintained at 5 $\pm$ 0.05 mm/min.

Selection of an initial sample position relative to the furnace such that about 2 cm of sample remains unmelted allows reliable identification of the start of unidirectional growth. The known solidification rate of the sample can then be correlated with accelerometer data to determine the gravity level during solidification for any location on the sample. For the typical parabola when entering low-g, the acceleration drops from 1 g to 10^{-2} g in less than 1.5 sec. For convenience in the figures, a low-g zone represents the time difference from when the system just went under 1 g going into low gravity to when it just went over 1 g coming out of low gravity.

C. Compositions Chosen for Study

The compositions chosen for study are shown in Figure 1 relative to the Al-In-Sn immiscibility dome [23]. Five hypermonotectic compositions were studied with Sn content from 0 to 22 wt.%. Their initial "nominal" compositions were (in wt.%) Al-18.6In, Al-30.0In, Al-18.5In-6.6Sn, Al-18.9In-14.6Sn, and Al-18.1In-22.0Sn. In some of the figures and text the compositions are referred to by the integer values of the weight percent for convenience.

D. Sample Preparation

The samples were prepared by placing the appropriate weights of five nines pure indium and tin, and four nines pure aluminum into a 99.8 percent alumina crucible. The sample was then melted under argon using an electromagnetic furnace. After about 10 min at about 1000°C the sample was quenched by aspirating it into a 4 mm id quartz tube.

After quenching, the samples were broken out of the quartz tubes and 1 cm was cut from the top for chemical analysis. Atomic adsorption analysis indicated that all the specimens were hypermonotectic and within 1.3 wt.% of the nominal tin content.

E. Quantitative Microscopy

Quantitative microscopy was used to obtain data on the change in volume fraction of the In or In-Sn-rich phase with solidification distance. An Omnicon image analysis system and enlarged photomicrographs were used for this purpose. This technique was chosen for the initial analysis over wet chemical analysis because the nondestructive nature of the former technique allowed subsequent electronic properties measurements which are described in another paper [24].

Area fraction of the dark In or In-Sn-rich phase was measured. It was assumed that the volume fraction was equal to the area fractions measured. Each measurement shown in the figures represents the average volume fraction of an area about 3 mm wide (perpendicular to the longitudinal axis) and 0.3 mm long (parallel to the longitudinal axis).

III. EXPERIMENTAL RESULTS

A. Directional Solidification Under Normal Gravity

The directionally solidified Al-30In samples often exhibited gross segregation of the In-rich-phase near the beginning of unidirectional growth. Figure 2 shows a typical sample in which the first millimeter after the start of unidirectional growth (SUG) consisted of an indium-rich band. Indium-rich metal also coated portions of the outside of the unmelted region of the sample. This run down of indium-rich liquid could result in only a broken band of indium-rich metal at the start of unidirectional growth (as occurred in the Al-30In flight sample shown later). The remainder of the Al-30In sample in Figure 2 consists of irregular shaped indium-rich particles dispersed in an aluminum-rich matrix. This latter microstructure is essentially that expected [4] for the monotectic composition solidified at the G and R used in this study.

Figure 3 shows photomicrographs of longitudinal sections of the four other compositions after directional solidification. The Al-18In sample in contrast to the Al-30In sample did not form a complete band of indium-rich metal at SUG. Instead, the first few millimeters of unidirectional solidified sample consists of indium-rich fibers aligned to the growth direction. This fibrous section consists of a few fibers of about 0.1 mm thickness and numerous finer fibers. The fibrous growth ends abruptly after about 2 mm; the microstructure then consists of irregular indium-rich particles dispersed in an aluminum-rich matrix with some intermittent aligned fibers occurring after about 4 mm of unidirectional growth. Figure 4 shows photomicrographs of transverse sections across the aligned fibers at 1.5 mm from SUG and the irregular indium-rich particles at 6.5 mm from SUG. The transverse section (Fig. 4A) reveals that the finer fibers are grouped in bands of about 50 microns thick and 100 microns spacing, while the larger fibers do not appear to have a regular spacing. The volume fraction indium-rich phase versus distance from SUG obtained from quantitative microscopy is given in Figure 5 for the Al-18In composition. It is clear that the composition of the fibrous portion of the sample is indium-rich relative to the rest of the sample. The indium content of the first fibrous band increases with solidification distance reaching a maximum of about 30 volume percent and then abruptly decreasing below that of the nominal composition at the end of the first fibrous region. The volume fraction In increases again at a position corresponding to regions of intermittent fibers.

The longitudinal section for the Al-18In-6Sn sample (Fig. 3) shows In-Sn-rich phase near SUG in the form of irregular macrodroplets somewhat oriented to the growth direction. At 3 mm from SUG there appears a partial band of lens-shaped droplets. After 3 mm irregular In-Sn-rich particles gradually are replaced by aligned spheres and then by aligned fibers at about 8.5 mm from SUG. The aligned fibers end abruptly and the remaining sample consists of irregular In-Sn-rich particles in an Al-rich matrix. Figure 6A shows a transverse section of the aligned fibers at 8.5 mm from SUG contrasted with (Fig. 6B) the irregular structure at 11 mm from SUG. In place of the fine irregular structures in Figure 6B are groupings of regularly spaced fibers in Figure 6A surrounded by a coarser microstructure that is common to both sections. Figure 7 gives the volume fraction change with distance from SUG for the Al-18In-6Sn sample. The volume fraction In-Sn-rich phase peaks well above the nominal composition in the area of the particle band of lens-shaped droplets (3 mm from SUG). Another increase occurs as the fraction of the sample consisting of aligned spheres increases. A sharp drop in measured volume fraction precedes the transformatin to aligned fibers.

The longitudinal section for Al-18In-14Sn (Fig. 3) shows large irregular-shaped macrodroplets in the first few millimeters after SUG. The microstructure then consists of irregular In-Sn-rich particles in an Al-rich matrix until at about 6 mm from SUG a concentrated band of irregular macrodroplets and fibers is evident ending at 8 mm from SUG in a band of lens-shaped droplets. The remainder of the sample consists of irregular In-Sn particles. Figure 8A shows a transverse section of the band of droplets at 8 mm from SUG. The macrodroplets are seen to form a somewhat regular pattern. The coarser connected microstructure of the transverse section at 10 mm from SUG (Fig. 8B) is common to both sections. The quantitative microscopy for the 14Sn sample, Figure 9, shows that the two regions dominated by macrodroplets correspond to dramatic increases in volume fraction of In-Sn-rich phase.

The Al-18In-22Sn sample (Fig. 3) did not exhibit the macrodroplets that were prominent in the 6Sn and 14Sn samples. Instead, intermittent large (0.05 mm) fibers begin at about 2 mm from SUG and continue to about 5 mm from SUG. Figure 10 shows a transverse section of the fibrous region at 4.5 mm from SUG contrasted with the irregular microstructure at 7 mm from SUG. It is apparent that the fibers are regularly spaced except for fiberless gaps. The quantitative microscopy (Fig. 11) shows an increase in volume fraction In-Sn-rich phase with the start of fibrous growth but a decrease is not evident in volume fraction after fibrous growth ceases at 55 mm from SUG.

B. Directional Solidification During Low-Gravity Maneuvers

Figure 12 shows longitudinal sections of Al-18In and Al-30In samples that were solidified during KC-135 low-gravity maneuvers. The Al-18In sample has a 1 mm band of aligned fibers that begins at about the middle of the first low-g zone and ends abruptly slightly before the end of the first low-g zone. The remainder of the sample consists of irregular particles of In-rich phase in Al-rich matrix with no obvious microstructural correlation to the gravity level at solidification. The microstructure of the Al-30In sample is similar to that of the Al-18In flight sample except that aligned fibers appear immediately after SUG and are followed by macrodroplets. Like the Al-18In flight sample the remaining sample is dominated by irregular In-rich particles that start before the end of the first low-g zone. Figure 13 gives the volume fraction versus distance from SUG for the Al-30In sample. It is evident that the volume fraction In-rich phase near SUG is greatly enriched in indium over the nominal composition but then drops quickly with distance from SUG.

A longitudinal section of Al-18In-6Sn flight sample is given in Figure 14. There is an interesting contrast in the segregation behavior of the 6Sn flight sample with that of the 0Sn flight samples. Whereas for 0Sn the excess In-rich phase appears in the first low-g zone, the 6Sn sample does not have macrodroplets until the beginning of the first high-g period. Quantitative microscopy (Fig. 15) shows that the volume fraction In-Sn-rich phase remains essentially the same as it was before SUG throughout the first low-g zone, then increases rapidly with the onset of high-g peaking at over 60 volume percent and then returning to the level before SUG by the middle of the first high-g zone to remain at that level for the rest of the sample.

Al-18In-14Sn samples like the 6Sn samples also did not have macrodroplets in the microstructure until the first high-g zone. For some samples for each Sn composition, furnace translation was stopped after 10 sec or less of the first high-g zone and then solidification was continued only in low-g for the next four maneuvers before returning to continuous solidification in low- and high-g. No new information was apparent for the 0Sn and 22Sn compositions from using this procedure, however, some interesting results were obtained for the 6Sn and 14Sn compositions. For the 6Sn and 14Sn compositions, when this procedure was followed, it was found that the excess L_2 could be made to incorporate more gradually in smaller macrodroplets by shortening the solidification time in high-g. For the 6Sn sample some of the smaller macrodroplets incorporated in low-g zones.

When the 14Sn alloy was processed using this procedure the excess In-Sn-rich phase did not appear to incorporate except at or immediately following high gravity as is evident in the irregular macrodroplets in the 14Sn sample in Figure 14. Unlike the lower Sn flight samples, the 14Sn sample also exhibited a second band of macrodroplets on the transition from the second high-g zone to the third low-g zone. This band of macrodroplets is similar to that in the ground 14Sn sample at 8 mm from SUG that abruptly terminated the macrodroplet microstructure. A comparison of Figure 9 with Figure 16 shows that the volume fraction In-Sn-rich phase of the two bands of droplets is about 40 volume percent.

The Al-18In-22Sn flight sample like the 22Sn ground sample did not exhibit macrodroplets. The microstructure of the 22Sn flight samples remained irregular In-Sn-rich particles dispersed in an Al-rich matrix throughout solidification through the first several parabolas. Beginning at about the fourth maneuver, an abrupt difference in microstructure between the material solidified in low-g and high-g becomes evident. Figure 17 shows the microstructure at the transition between the fourth low- and high-g zones. By inspection of Figure 17 it is evident that the In-Sn particles in the low-g zone are finer and tend to be more aligned. Figure 18 shows a longitudinal section spanning the area from the third to the fourth high-g zones of the flight sample and the corresponding section of a control sample solidified under the same conditions except for gravity. It is evident from such comparisons that the change in microstructure is a function of gravity level during solidification and distance from SUG. A comparison of the transverse microstructure for high-g and low-g is given in Figure 19.

A finer microstructure and greater degree of alignment in the low-g microstructure is also evident but to a lesser degree in the transverse sections. Figure 20 gives the volume fraction versus distance from SUG corresponding to the section of the flight sample shown in Figure 19. An abrupt decrease in volume fraction In-Sn-rich phase is evident at the beginning of low-g coinciding with the aligned irregular microstructure. The volume fraction then increases steadily through the low-g zone falling sharply again at the low-g to high-g transition.

IV. DISCUSSION

A. Segregation of Excess L_2 Under a Thermal Gradient in a Gravitational Field

To interpret the results of these experiments it is critical first to understand the segregation that takes place in a hypermonotectic melt standing in a thermal gradient relative to a gravitational field [25]. Figure 21 is an illustration of this situation with L_2 more dense than L_1 as is the case for the systems in this study. Since the system (Fig. 21A) is hypermonotectic, the temperature gradient results in a band of liquid that exists in the temperature range that falls in the immiscibility dome (Fig. 21B). Stokes settling of the L_2 droplets to the solid + L_2 interface occurs due to gravity. The composition of the liquid above the L_2-rich band at the interface is continually homogenized, due to convective flows, resulting in nucleation of L_2 droplets in the temperature gradient zone. The process continues until the composition of the liquid above the L_2-rich region at the solid + L_2 interface reaches the monotectic composition (Fig. 21B). If the system is rich enough in component B then the droplets of L_2 at the interface merge to form a continuous band at the solid + L_2 interface (Fig. 21C). When the sample is translated relative to the thermal gradient, to begin growth, unless R is slow relative to diffusion of solute through the L_2 band, growth will be interrupted and begin after the L_2 band is passed. The Al-30In microstructure given in Figure 2 is an example of this phenomenon. Other examples are in the literature for Al-In [4] and for Cu-Pb [7]. Since growth is interrupted at practical rates, experiments at these compositions yield little information about the behavior of excess L_2 at the growing interface. The "slightly-hypermonotectic" compositions Al-18In, Al-18In-6Sn, Al-18In-14Sn, and Al-18In-22Sn were selected for study because the concentration of B apparently was not great enough to cause droplets of L_2 at the solid + L_2 interface to merge into a band, Figure 21C. In this way the effect of variables such as disjoining pressure and gravity on the incorporation of excess L_2 in the growth front could be studied.

B. The Effect of Gravity on the Integration of Primary Macrodroplets

The mechanisms of integration of L_2 into the solidifying interface for Al-In alloys has been the subject of some controversy in the literature. Grugel and Hellawell [4] found that monotectic Al-In alloys solidified in regular aligned composite structures at high G/R. They assumed based on the arguments of Cahn [3] that L_2 wet the solid. Derby and Favier and Derby [6,26] tested this assumption by interfacial energy calculations and concluded that L_1 preferentially wets the solid; thus, this assumption is invalid. They suggested that dynamic wetting theory of Chernov et al. [27] be applied. Potard [8] compared the results of Bridgman and capillary tube quench solidification experiments with hypermonotectic Al-In and concluded that under conditions that particle inertia becomes negligible, only the weight of the primary globules enables them to overcome the interfacial repellent force and integrate into the solid. Potard [12] also solidified hypermonotectic Al-In in low gravity in a sounding rocket experiment and observed that primary particles well above the size that Chernov's theory predicts appeared to experience repulsion by the solidification interface during solidification in low gravity.

Figure 22 is a schematic of the macrostructure found in the flight and ground samples for the Al-In-Sn compositions studied. The results for the 6Sn and 14Sn compositions support Potard's finding from sounding rocket results that large primary droplets can be repelled by the solidification front when gravity is absent. We did not, however, observe a notable difference as a function of gravity in the primary phase integration for Al-18In or Al-30In compositions. We instead saw an increased sensitivity in the influence of gravity on primary phase integration with increasing Sn content presumably due to increasing disjoining pressure at higher Sn content. The difference in observations for Al-In between the two low-gravity experiments might be due to the lower gravity (0.0001 g) for the sounding rocket experiment relative to that (0.01 g) in the KC-135 maneuver. The size of the primary particles apparently repulsed by the interface in both the KC-135 and sounding rocket low-gravity experiments is larger by at least an order of magnitude than would be expected from Chernov's dynamic wetting theory [6].

C. Compositional Dependence for the Formation of Aligned Composite Structure

Figure 3 shows that at normal gravity all the slightly hypermonotectic compositions studied exhibited aligned composite growth within the first centimeter from SUG. At first glance this seems to be in contradiction to the study of Grugel and Hellawell, since for monotectic compositions they observed only irregular In or In-Sn-rich particles in an aluminum-rich matrix at the G and R conditions of our study. Examination of the quantitative microscopy data (Figs. 5, 7, 9, and 11) reveals that the aligned structures are correlated with high volume fractions of In or In-Sn-rich phase — with hypermonotectic compositions. The surrounding microstructure which is close to monotectic composition is consistent with what would be expected at our growth conditions from Grugel and Hellawell's results. It is interesting to note that the banding of the aligned fibers in the Al-18In transverse section (Fig. 4A) is similar to that reported by Grugel and Hellawell for on monotectic Al-In at higher G/R. Livingston and Cline [1] found an analogous dependency of alignment of CuPb, for fixed G and R, with Pb content. Our study is to our knowledge the first to demonstrate that the tendency to form aligned composite microstructure for the Al-In-Sn system is a function of composition.

D. Spacings of Aligned Structures

Derby and Favier [6] extended the Jackson-Hunt diffusion theory to monotectic systems. Grugel and Hellawell [4] suggest that the $\lambda^2 R$ is a constant for monotectics where λ is the aligned structure spacing but that the constant depends on the height of the miscibility gap. Table 1 lists the spacings of aligned structures found in this study relative to values measured by Grugel and Hellawell for monotectic compositions of Al-In (regular fibrous) and Al-In-Sn (irregular fibrous). Most of the fibrous structures observed in this study are on the order of the irregular fibrous spacing found by Grugel and Hellawell. This suggests that the hypermonotectic aligned structures solidify by a mechanism similar to that of on monotectic irregular fibrous-type growth. Only the spacings measured for aligned spheres in Al-18In approach that of Grugel and Hellawell measurements for uniform fibrous Al-In. The quantitative microscopy data in Figure 7 show, however, that this microstructure was accompanied by a lowering of the indium volume fraction to near monotectic levels.

It is interesting to note that the spacings (Table 1) of the Al-In-22Sn aligned globules found in low-gravity solidification were essentially the same as the spacing of the large fibers found in the sample solidified at normal gravity. Also it should be noted that the spacings of these two aligned structures are substantially greater than any of the other structures listed in Table 1. The transverse sections for the ground (Fig. 10) and flight (Fig. 19) sample show evidence for cellular solidification. Figure 23 shows the spacing between aligned

globules found in low-gravity-solidified Al-18In-22Sn relative to the transverse section macrostructure. Systematic interfacial stability studies for the Al-In-Sn system have not been done but an extrapolation of data on the cell size versus 1/RG for Al-2Cu [28] to our growth conditions is consistent with the spacing values obtained for the Al-18In-22Sn aligned structures.

E. Interfacial Stability and Gravity Level

A deep etch of the band between the second high and third low-gravity zone in the 14Sn sample reveals that it is essentially different from the macrodroplets seen at the first high-g zone in the 14Sn sample and also in the 6Sn sample. The deep etch of the latter band in the 14Sn sample reveals a network of aligned fibers that suggests a change in solidification mechanism. In addition the position of the latter band in the 14Sn sample — the transition from the second high-g zone to the third low-g zone — makes it unlikely that the latter band in the 14Sn sample resulted from the same mechanism as the macrodroplets found in the first high-g zones. A more likely cause of this microstructure as well as the aligned globules found in low-g zones of the 22Sn sample is that these structures result form the decreased interfacial stability caused by low gravity as predicted by Lemaignan and Malmejac [29]. It would be expected that the higher Sn compositions would be more sensitive to low-gravity-induced interfacial instability, since as the Sn concentration is increased the resulting change in the phase diagram is expected to make the Al-In-Sn alloys more sensitive to constitutional supercooling [29]. The growth of intercellular or intergranular fibers in Al-In alloys has been noted previously [6]. The destabilization of the solidification interface by low-g to a more cellular form has been reported in a study of Fe-C-P alloys [22] directionally solidified in low-gravity maneuvers.

V. CONCLUSIONS

1. By selection of hypermonotectic composition such that only a partial band of L_2 forms at the solid + L_2 interface, Bridgman directional solidification can be used to study the integration of excess L_2 into the solidification interface.

2. The formation of aligned composite structures in the Al-In-Sn system is not only a function of G and R but also of the degree of departure from the monotectic composition.

3. The spacings of the aligned structures formed at hypermonotectic compositions were for the Al-18In, Al-18In-6Sn, and Al-18In-14Sn alloys on the order of that reported for irregular fibrous Al-In-Sn on monotectic. The spacings for the aligned structure for the ground and low-gravity-solidified 22Sn alloy were significantly larger and are on the order of that expected for cellular spacing for the growth conditions studied.

4. The influence of gravity on the integration of excess L_2 for hypermonotectic Al-In-Sn alloys increases as the monotectic dome height decreases. For Al-In alloys, gravity (above about 0.01 g) was not necessary for the integration of excess L_2 while for Al-18In-6Sn and Al-18In-14Sn alloys, L_2 did not integrate until high gravity was present.

5. The higher Sn (lower monotectic dome height) alloys, Al-18In-14Sn and Al-18In-22Sn, exhibited aligned structure that was associated with low gravity or the transition from high to low gravity, and with the position on the sample relative to the start of unidirectional growth. It is believed that these microstructures are the result of the tendency for low gravity to destabilize the solidification interface.

REFERENCES

1. Livingston, J. D., and Cline, H. E.: Trans. AIME, Vol. 245, 1969, pp. 351-357.

2. Knight, R. J., Li, C. Y., and Spencer, C. W.: Trans. AIME, Vol. 227, 1963, pp. 18-22.

3. Cahn, J. W.: Metall. Trans., Vol. 10A, 1979, pp. 119-121.

4. Grugel, R. N., and Hellawell, A.: Metall. Trans., Vol. 12A, 1981, pp. 669-681.

5. Derby, B., Camel, D., and Favier, J. J.: J. Crystal Growth, Vol. 65, 1983, pp. 280-285.

6. Derby, B., and Favier, J. J.: Acta. Metall., Vol. 31, 1983, pp. 1123-1130.

7. Bergman, A., Carlberg, T., Fredriksson, H., and Stjerndahl, J.: Materials Processing in Reduced Gravity Environment of Space. Proceedings of the Materials Research Society Annual Meeting, G. E. Rindone, ed., North-Holland, 1981, pp. 579-592.

8. Potard, C.: AIAA Paper No. 79-0173, New Orleans, LA, 1979.

9. Delves, R. T.: Brit. J. Appl. Phys., Vol. 16, 1965, pp. 343-351.

10. Lacy, L. L., and Otto, G. H.: AIAA Journal, Vol. 13, 1975, pp. 219-220.

11. Hodes, E., and Steeg, M.: Z. Flugwiss, Weltraumforsch, Vol. 2, 1978, pp. 337-341.

12. Potard, C.: Materials Processing in Reduced Gravity Environment of Space. Proceedings of the Materials Research Society Annual Meeting, G. E. Rindone, ed., North-Holland, 1981, pp. 543-552.

13. Kneissl, A., and Feshmeister, H.: Proc. Fifth European Symposium on Materials Sciences Under Microgravity. Results of Spacelab-1, Schloss Elmau, FRG, ESA SP-222, 1984, pp. 63-69.

14. Ang, C. Y., and Lacy, L. L.: ASTP Experiment MA-044, NASA TM X-64956, Marshall Space Flight Center, AL, 1975.

15. Gelles, S. H., and Markworth, A. J.: AIAA Journal, Vol. 16, 1978, pp. 431-438.

16. Carlberg, T., and Fredriksson, H.: Metall. Trans., Vol. 11A, 1980, pp. 1665-1676.

17. Ahloborn, H., and Lohberg, K.: Proc. Fifth European Symposium on Materials Sciences Under Microgravity. Results of Spacelab-1, Schloss Elmau, FRG, ESA SP-222, 1984, pp. 55-62.

18. Gelles, S. H.: Liquid Phase Miscibility Gap Alloys. MEA Al Experiments, Final Post Flight Report, NAS8-32952, NASA, MSFC, 1984.

19. Johnston, M. H., Curreri, P. A., Parr, R. A., and Alter, W. S.: Metall. Trans., Vol. 16A, 1985, pp. 1683-1687.

20. Lee, J. E., McCay, M. H., and Curreri, P. A.: Metall. Trans., 1986, in press.

21. Hendrix, J. C., Curreri, P. A., and Stefanescu, D. M.: AFS Trans., Vol. 92, 1984, pp. 435-458.

22. Stefanescu, D. M., Curreri, P. A., and Fiske, M. R.: Metall. Trans., Vol. 17A, 1986, pp. 1121-1130.

23. Campbell, A. N., Buchanan, L. B., Kuzmak, J. M., and Tuxworth, R. H.: J. Am. Chem. Soc., Vol. 74, 1952, pp. 1962-1966.

24. Wu, M. K., Ashburn, J. R., Curreri, P. A., and Kaukler, W. F.: Metall. Trans., 1986, submitted.

25. Grugel, R. N., Lagrasso, T. A., and Hellawell, A.: Materials Processing in Reduced Gravity Environment of Space. Proceedings of the Materials Research Society Annual Meeting, G. E. Rindone, ed., North-Holland, 1981, pp. 553-561.

26. Derby, B.: Proc. Fourth European Symposium on Materials Sciences Under Microgravity, Madrid, 5-8 April 1983, ESA SP-191, pp. 277-280.

27. Chernov, A. A., Temkin, D. E., and Mel'nikova, A. M.: Sov. Phys. Crystallogr., Vol. 21, 1976, p. 369.

28. Sharp, R. M., and Hellawell, A.: J. Crystal Growth, Vol. 6, 1970, p. 335.

29. Lemaignan, C., and Malmejac, Y.: Materials Sciences in Space With Application to Space Processing, L. Steg, ed., American Institute of Aeronautics and Astronautics, NY, 1977, pp. 447-454.

30. Delves, R. T.: Brit. J. Appl. Phys., Vol. 16, 1965, pp. 343-351.

TABLE 1. SPACING OF ALIGNED COMPOSITE STRUCTURE

System	Gravity Level	Structure	$\lambda^2 v(M^3/S \times 10^{-14})$
Al-18In	Normal	Fibrous Band	2.05
Al-18In	Low	Fibrous Band	4.45
Al-30In	Low	Fibrous Band	3.71
Al-18.5In-6.6Sn	Normal	Fibrous Band	1.92
Al-18.9In-14.6Sn	Normal	Fibroud Band	1.05
Al-18.1In-22Sn	Normal	Fibrous Band	30.5
Al-18.1In-22Sn	Low	Aligned Globules	33.7
Al-18In	Normal	Aligned Spheres	0.21
Al-In-Sn (Grugel and Hellawell	Normal	Irregular Fibrous	5.30
Al-In (Grugel and Hellawell)	Normal	Uniform Fibrous	0.04

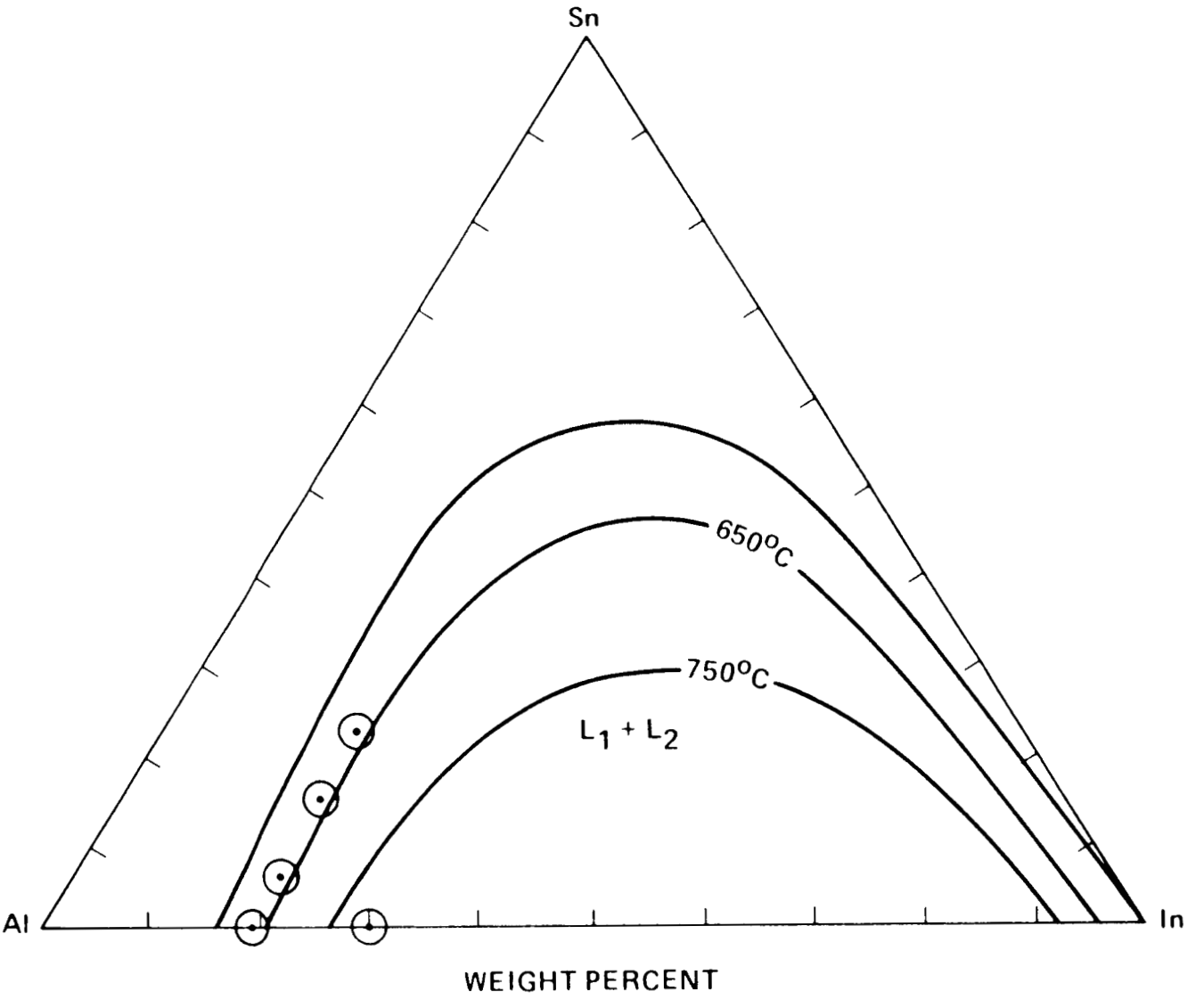

Figure 1. Al-x.In-y.Sn immiscibility dome after Reference 23. The circled points denote the compositions studied.

Figure 2. Al-30In sample showing the disruption of the solidification process by an indium-rich band near the start of unidirectional growth.

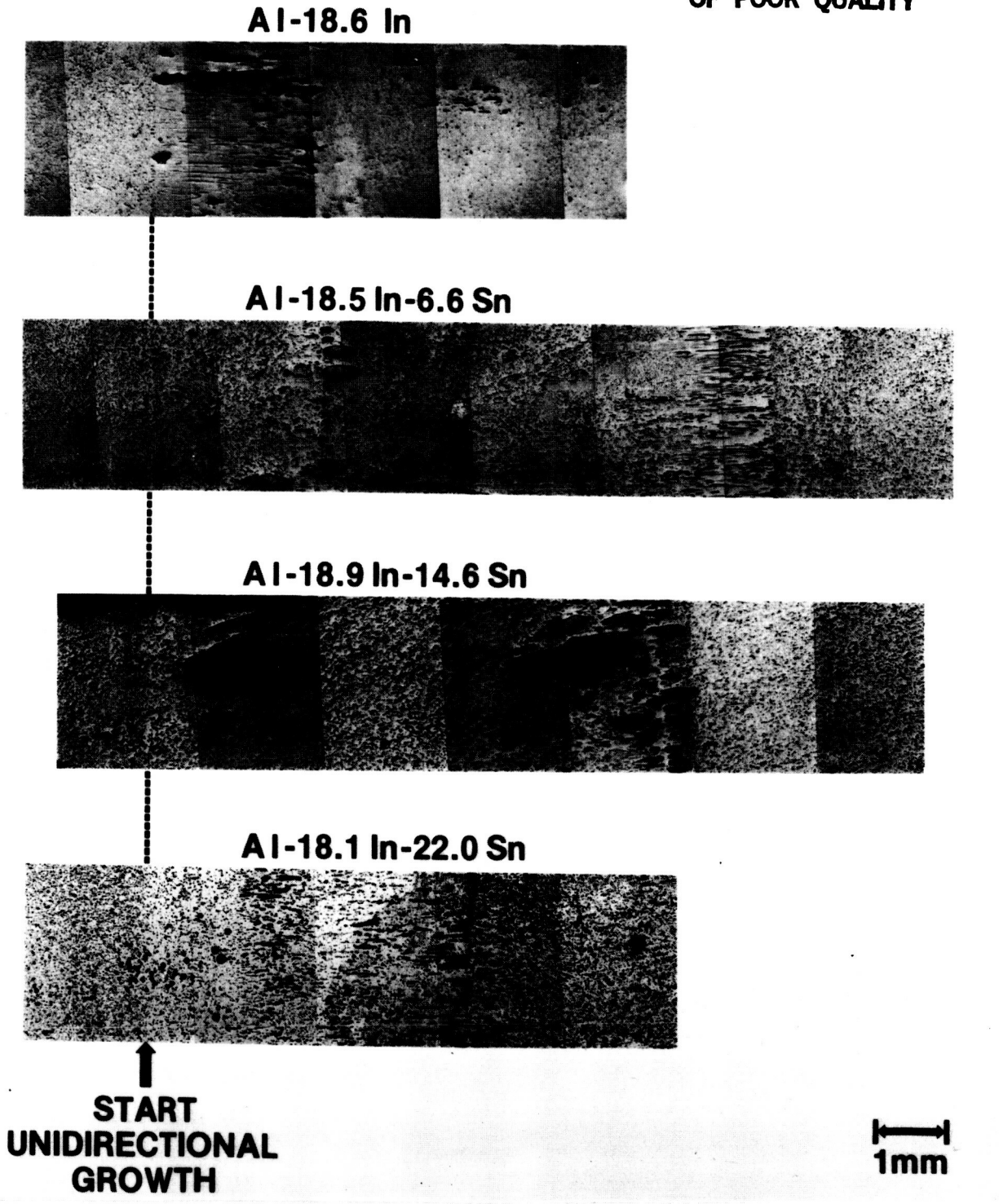

Figure 3. Hypermonotectic Al-x.In-y.Sn alloys directionally solidified upwards under normal gravity (ground). G = 250°C/cm; R = 0.5 cm/min.

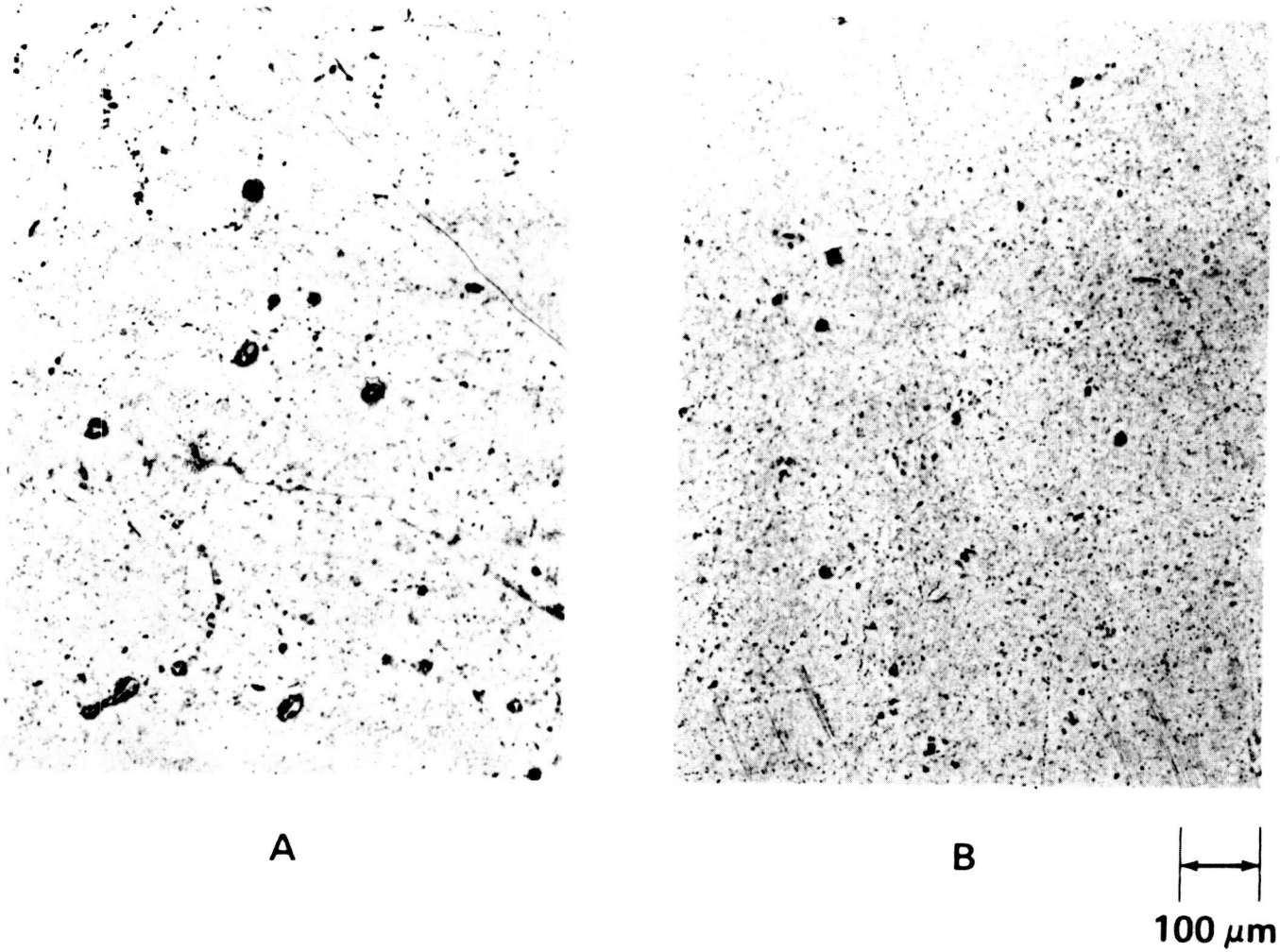

Figure 4. Transverse sections for Al-18.6In ground sample. (A) Aligned fibers at 1.5 mm from the start of unidirectional growth. (B) Microstructure at 6.5 mm from the start of unidirectional growth.

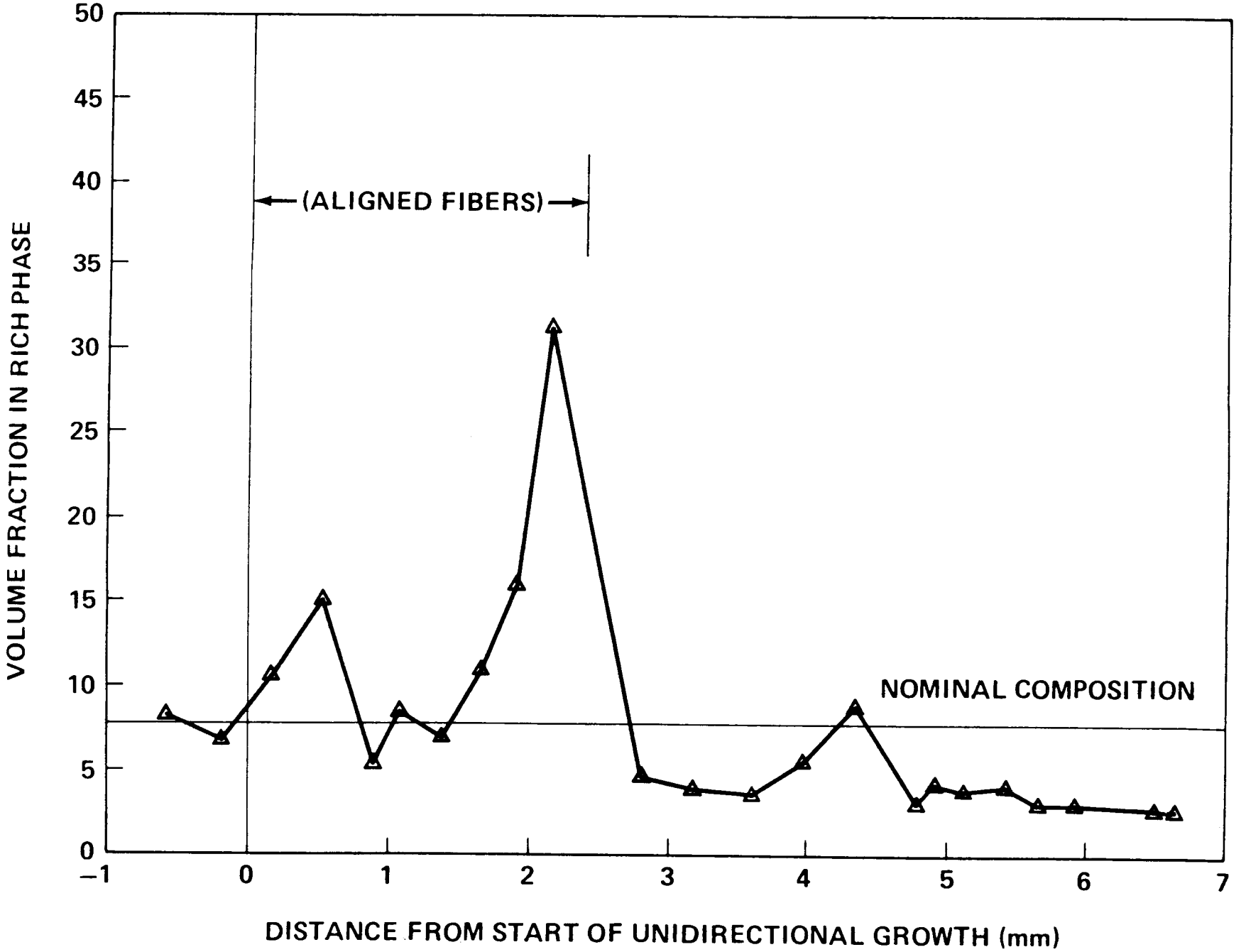

Figure 5. Quantitative microscopy for Al-18.6In ground sample.

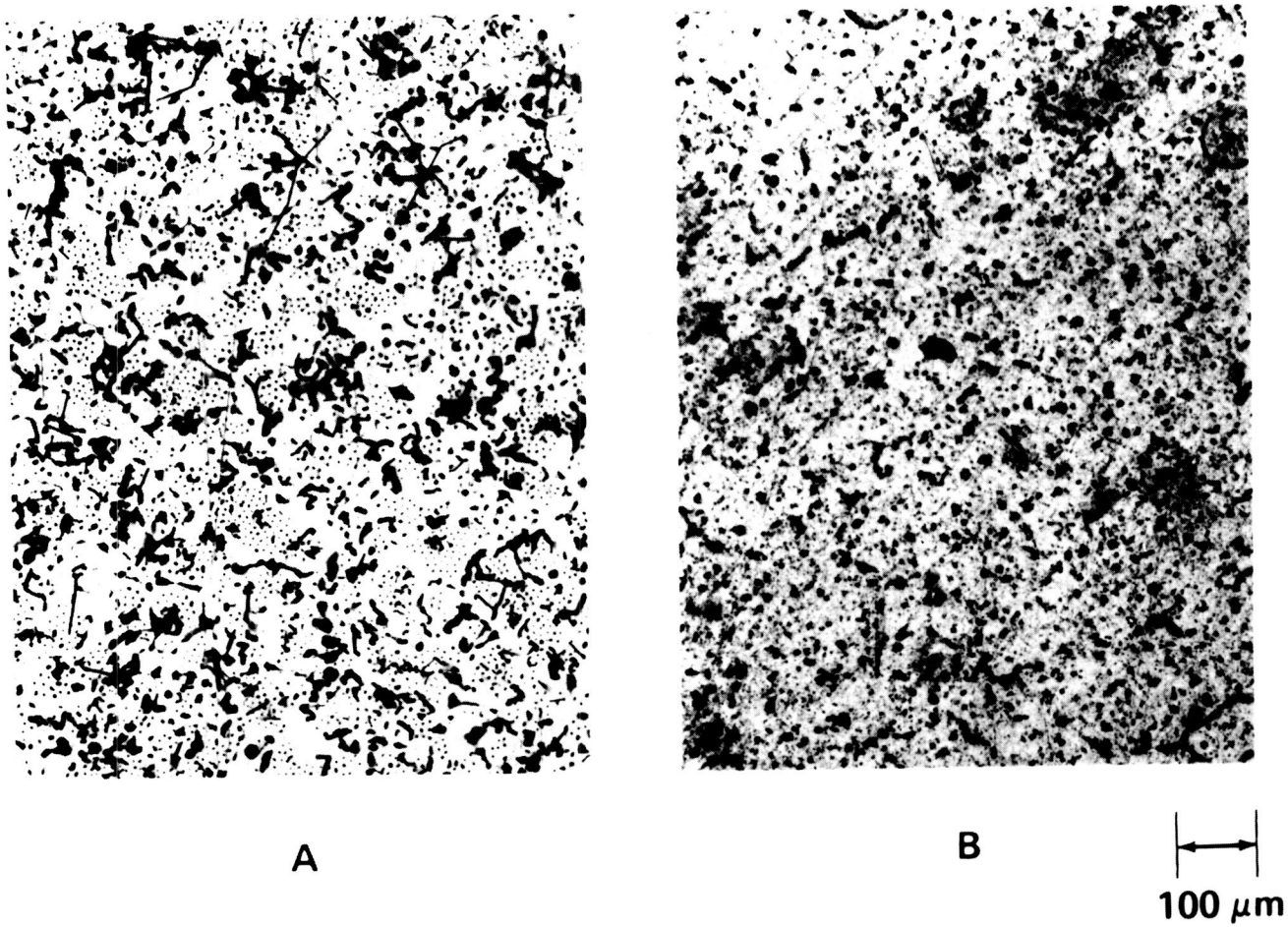

Figure 6. Transverse sections for Al-18.5In-6.6Sn ground sample. (A) Aligned fibers at 8.5 mm from the start of unidirectional growth. (B) Microstructure at 11 mm from the start of unidirectional growth.

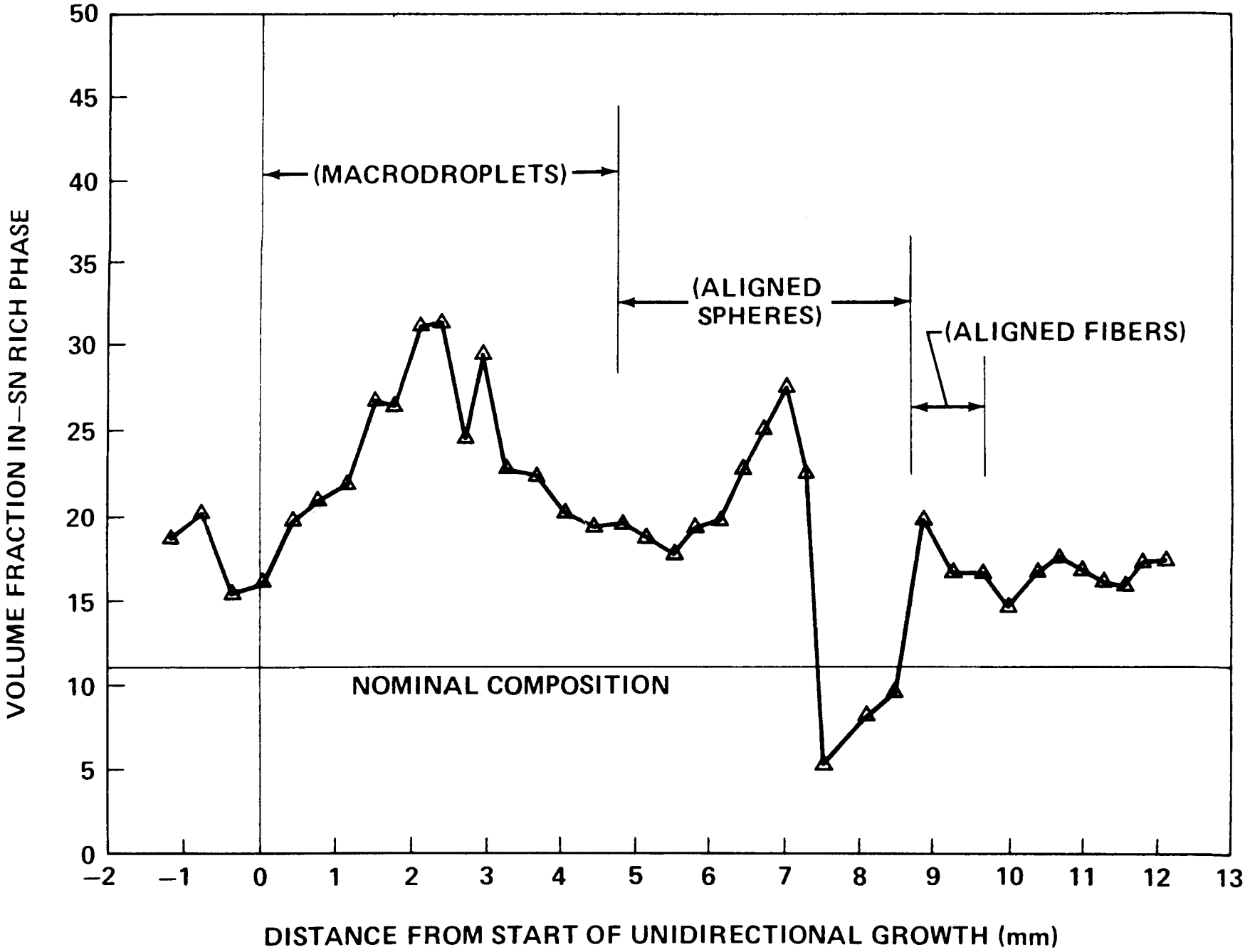

Figure 7. Quantitative microscopy for Al-18.5In-6.6Sn ground sample.

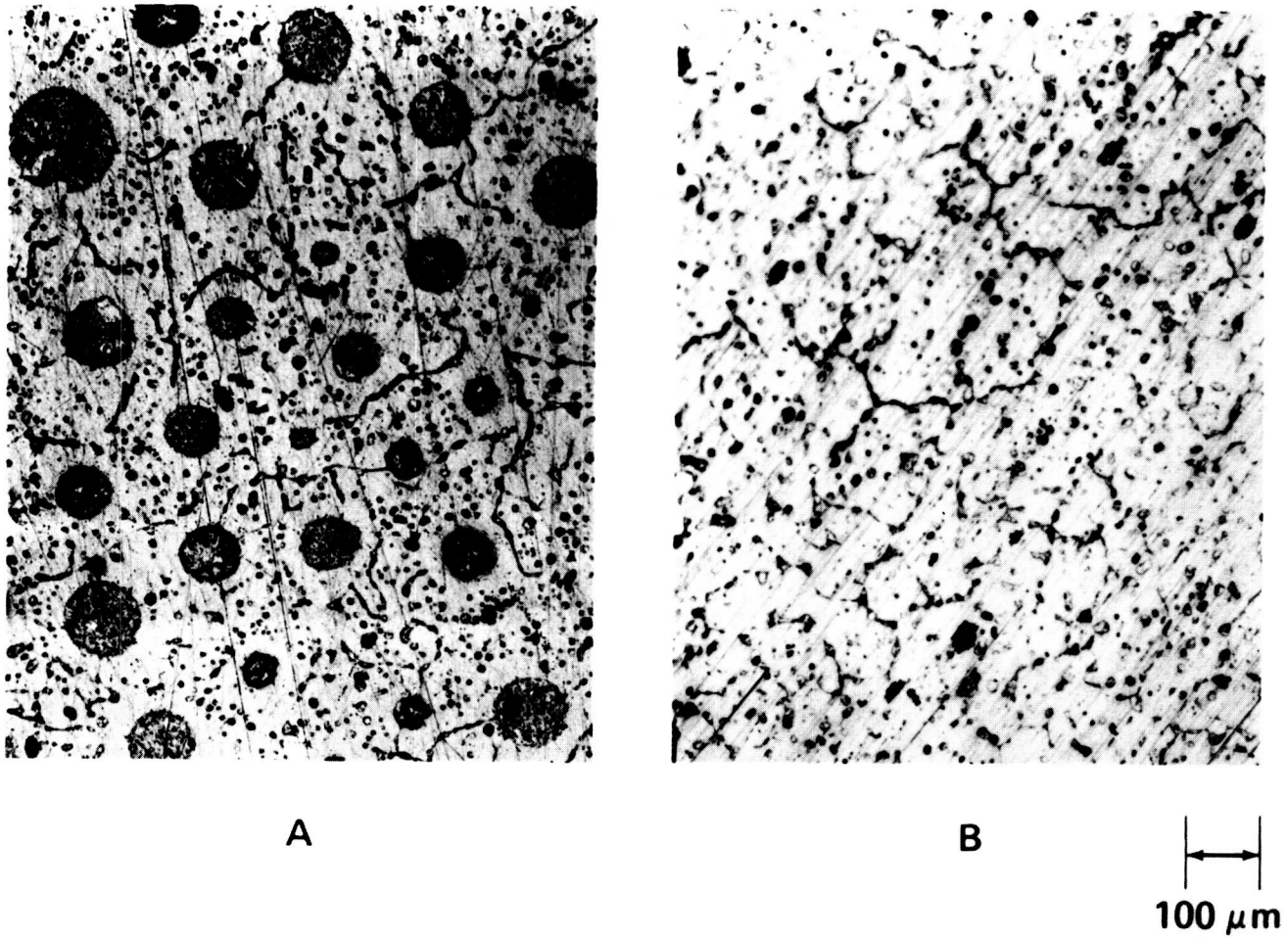

Figure 8. Transverse sections for Al-18.9In-14.6Sn ground sample. (A) Macrodroplets with aligned fibers at 7 mm from the start of unidirectional growth. (B) Microstructure at 10 mm from the start of unidirectional growth.

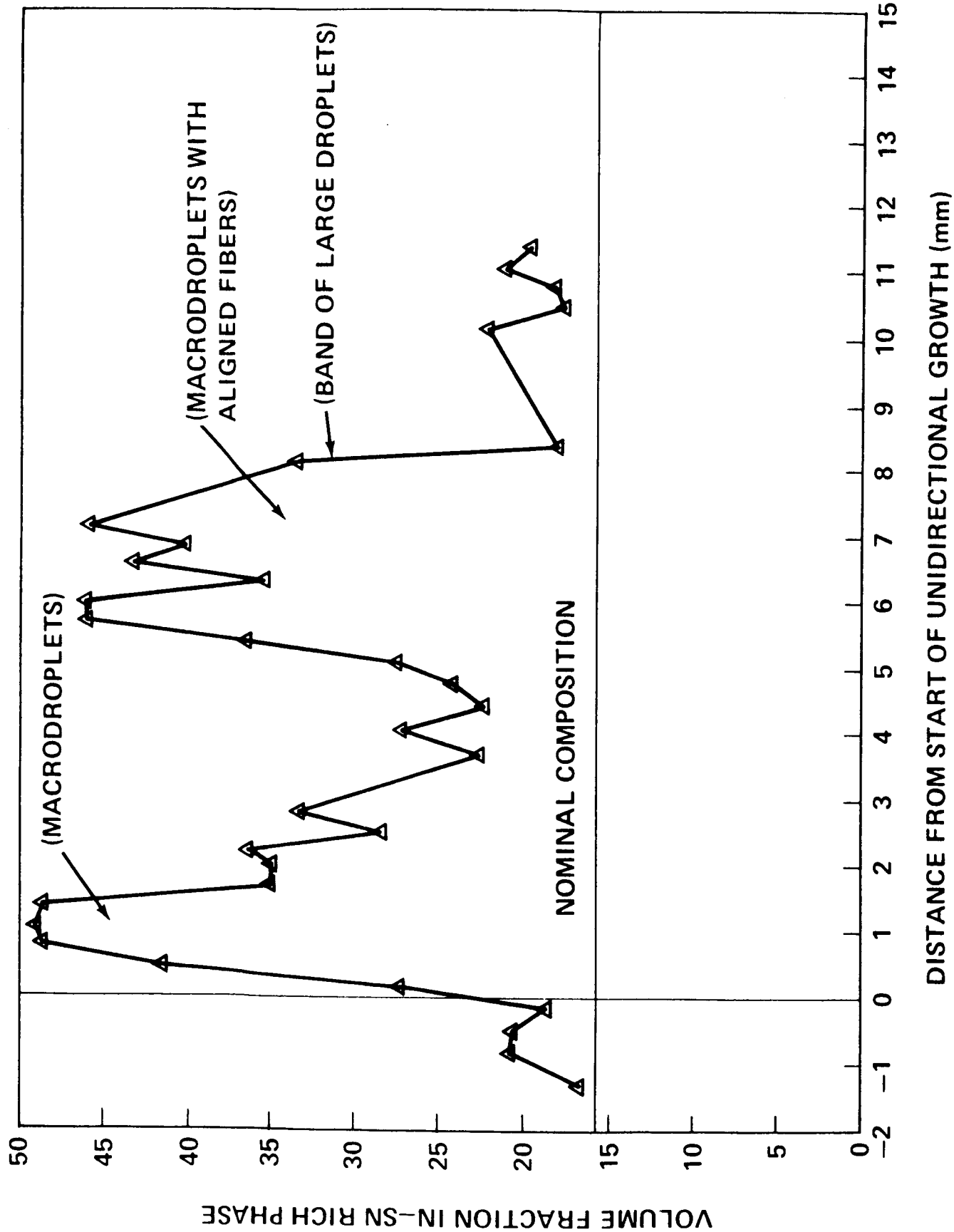

Figure 9. Quantitative microscopy for Al-18.9In-14.6Sn ground sample.

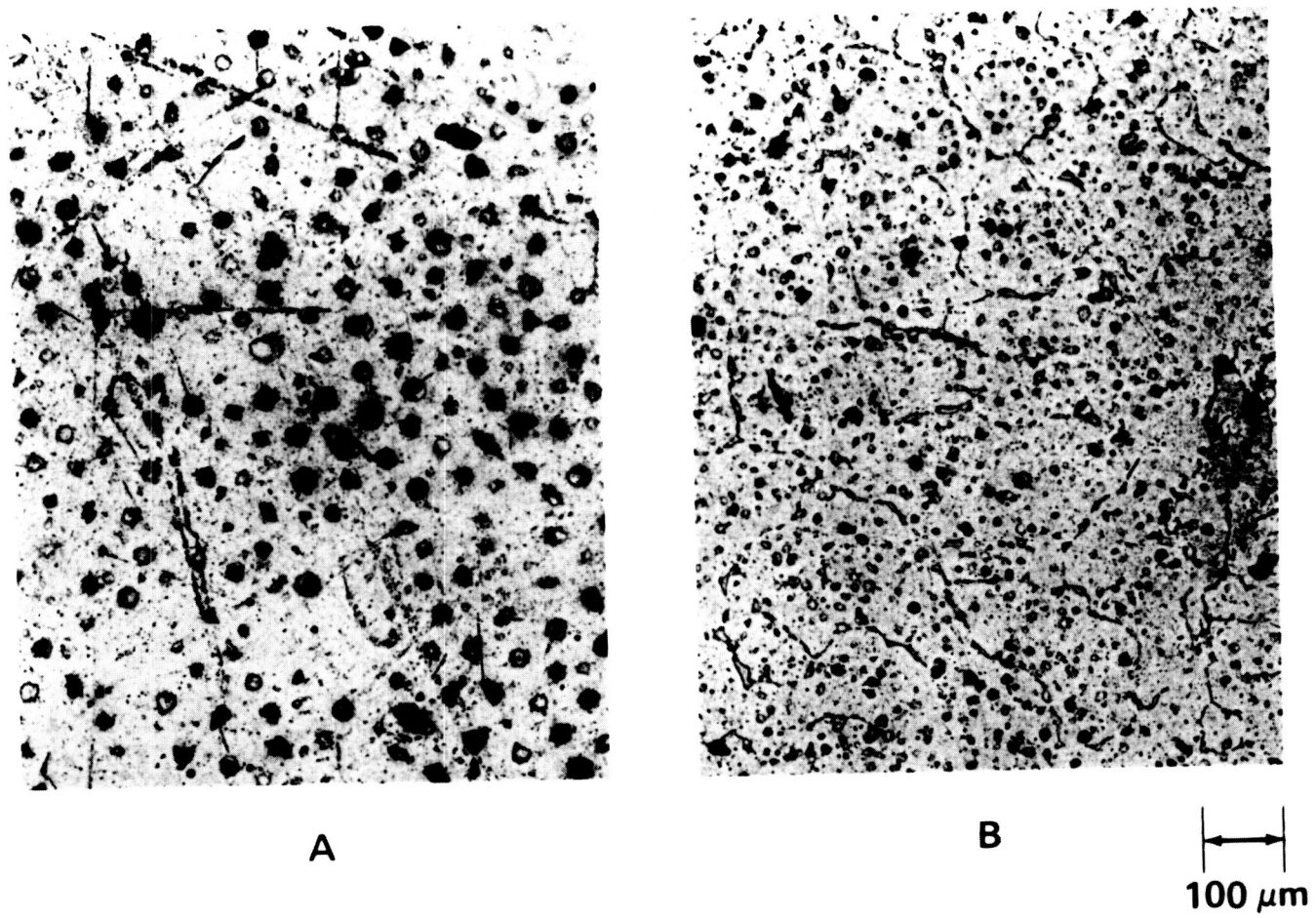

Figure 10. Transverse sections for Al-18.1In-22Sn ground sample. (A) Aligned fibers at 4.5 mm from the start of unidirectional growth. (B) Microstructure at 7 mm from the start of unidirectional growth.

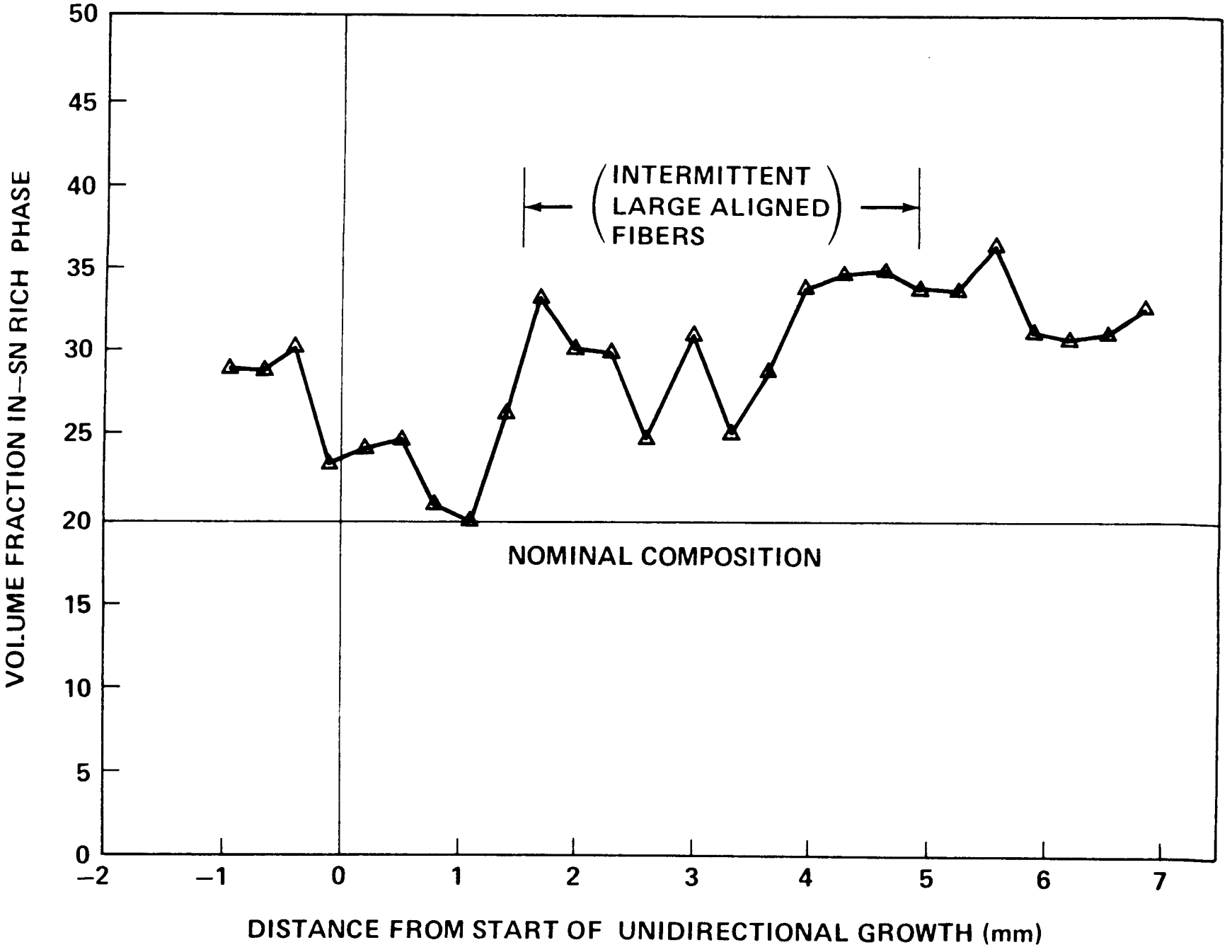

Figure 11. Quantitative microscopy for Al-18.1In-22Sn ground sample.

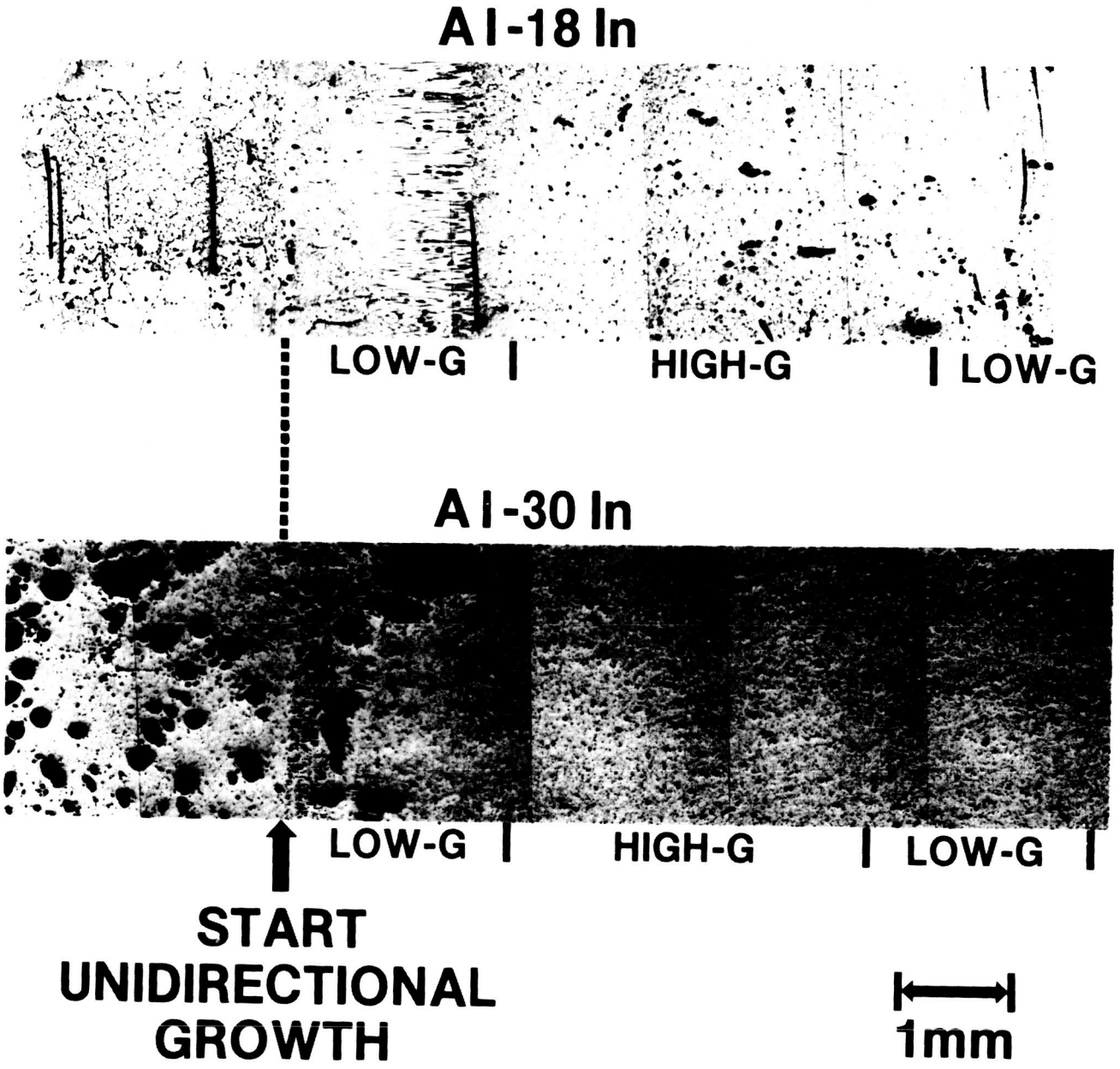

Figure 12. Hypermonotectic Al-x.In alloys directionally solidified during KC-135 maneuvers (flight). G = 250°C/cm; R = 0.5 cm/min.

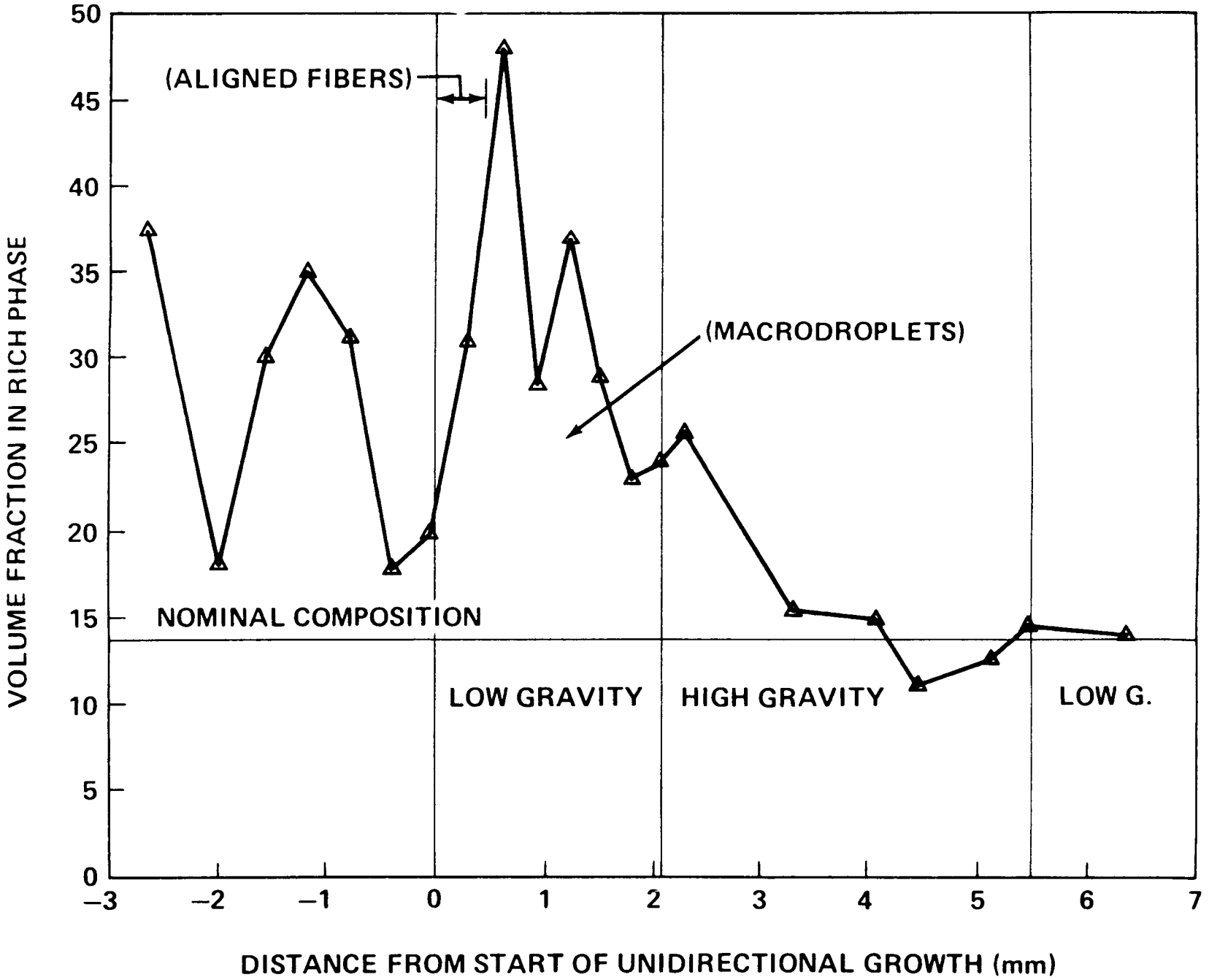

Figure 13. Quantitative microscopy for Al-30In flight sample.

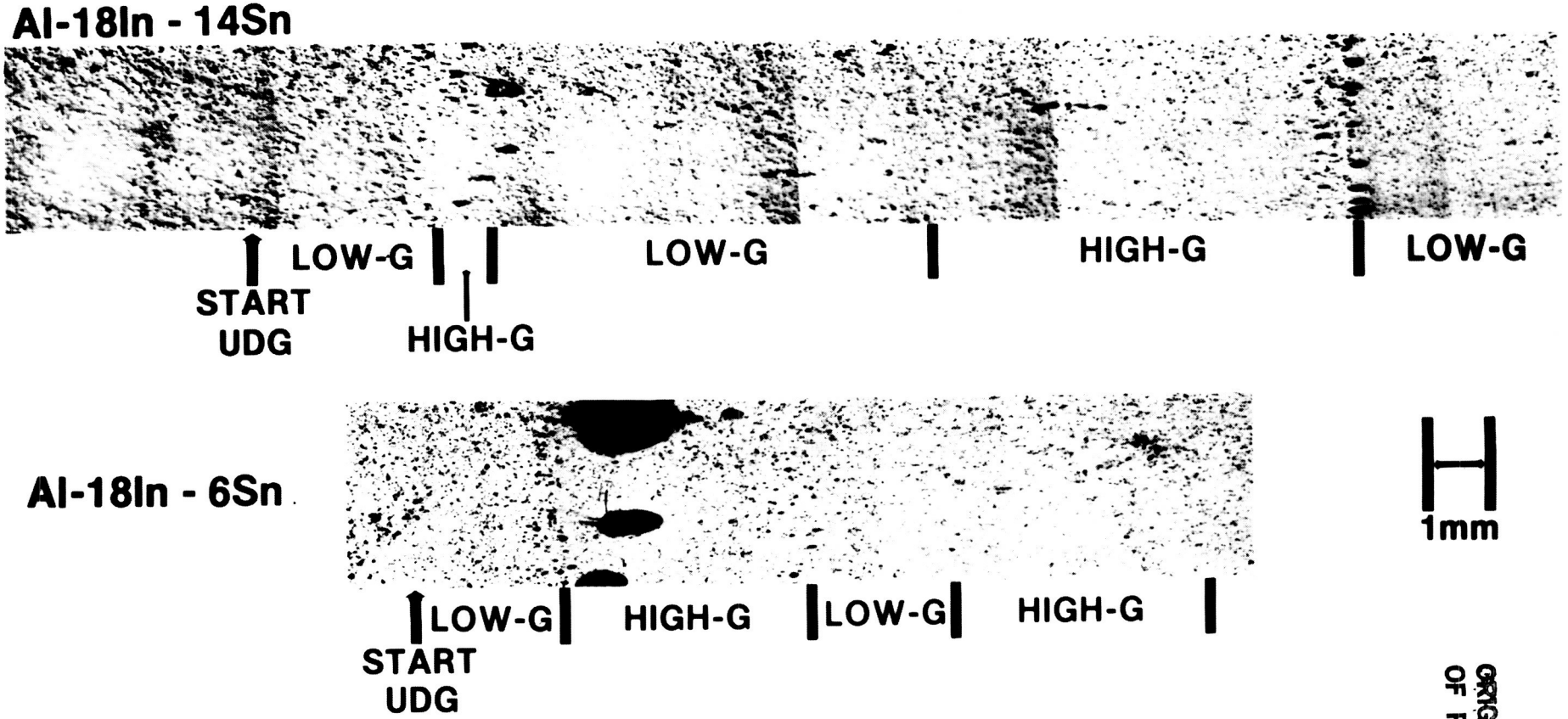

Figure 14. Hypermonotectic Al-18.5In-6.6Sn and Al-18.9In-14.6Sn flight samples. G = 250°C/cm; R = 0.5 cm/min.

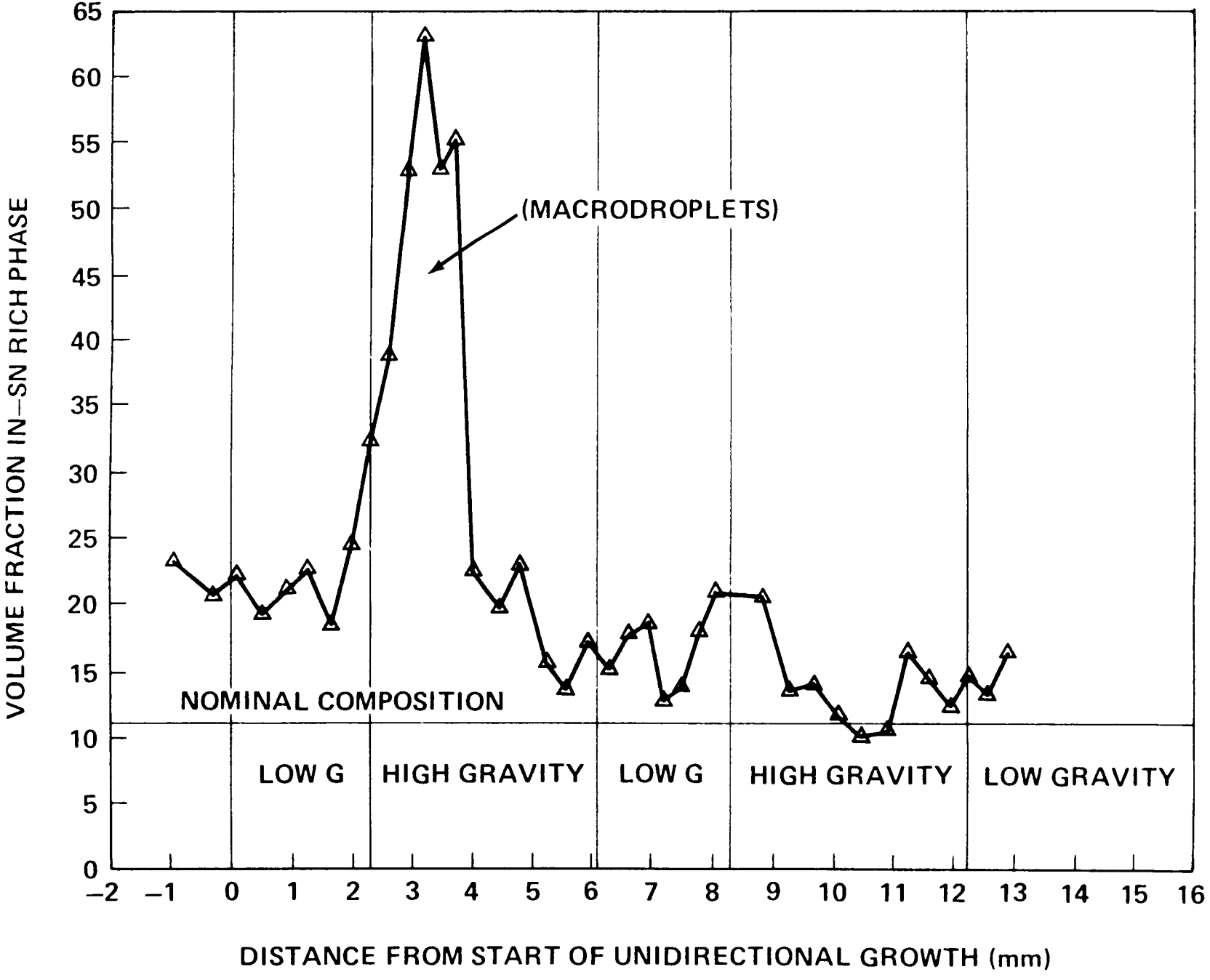

Figure 15. Quantitative microscopy for Al-18.5In-6.6Sn flight sample.

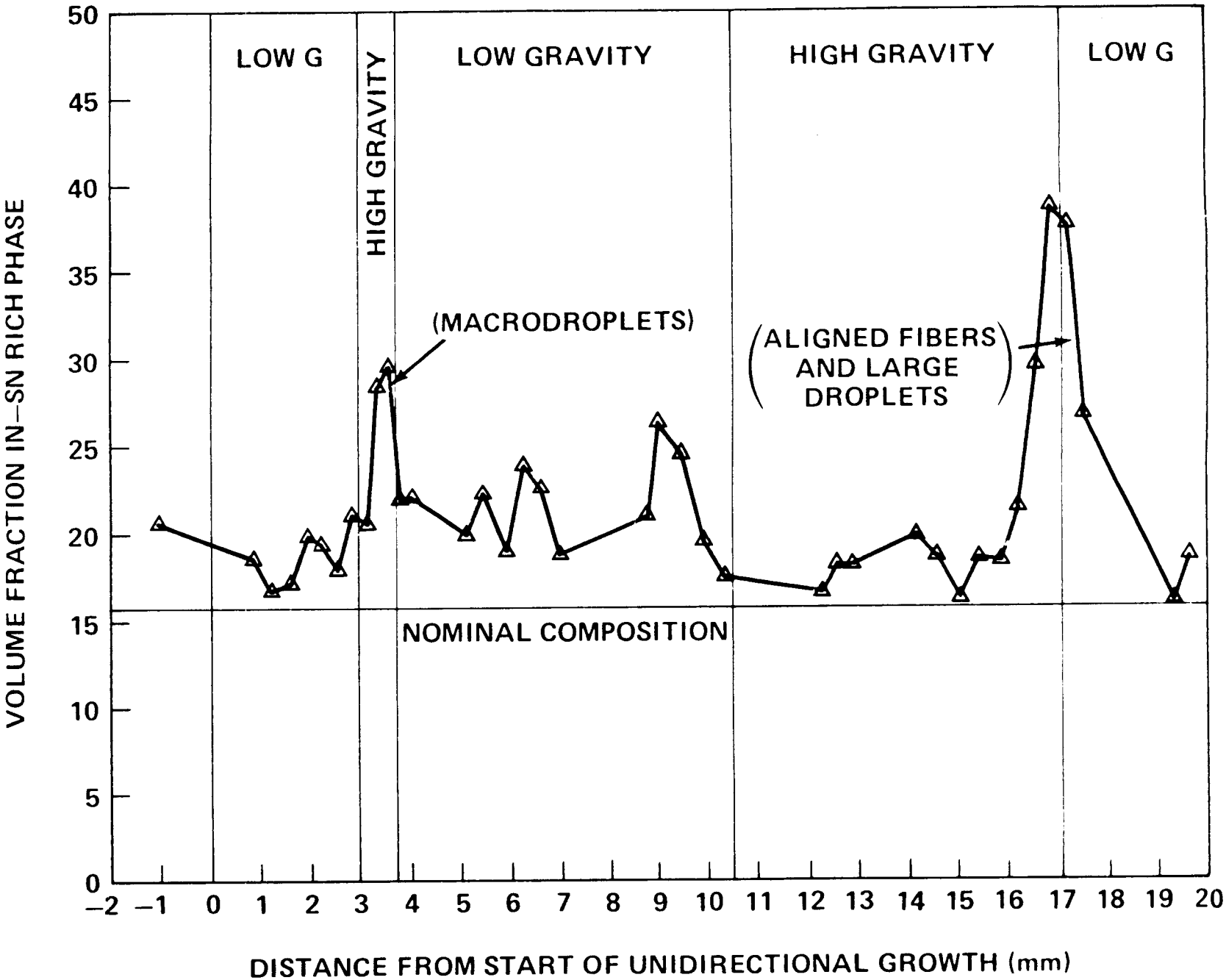

Figure 16. Quantitative microscopy for Al-18.9In-14.6Sn flight sample.

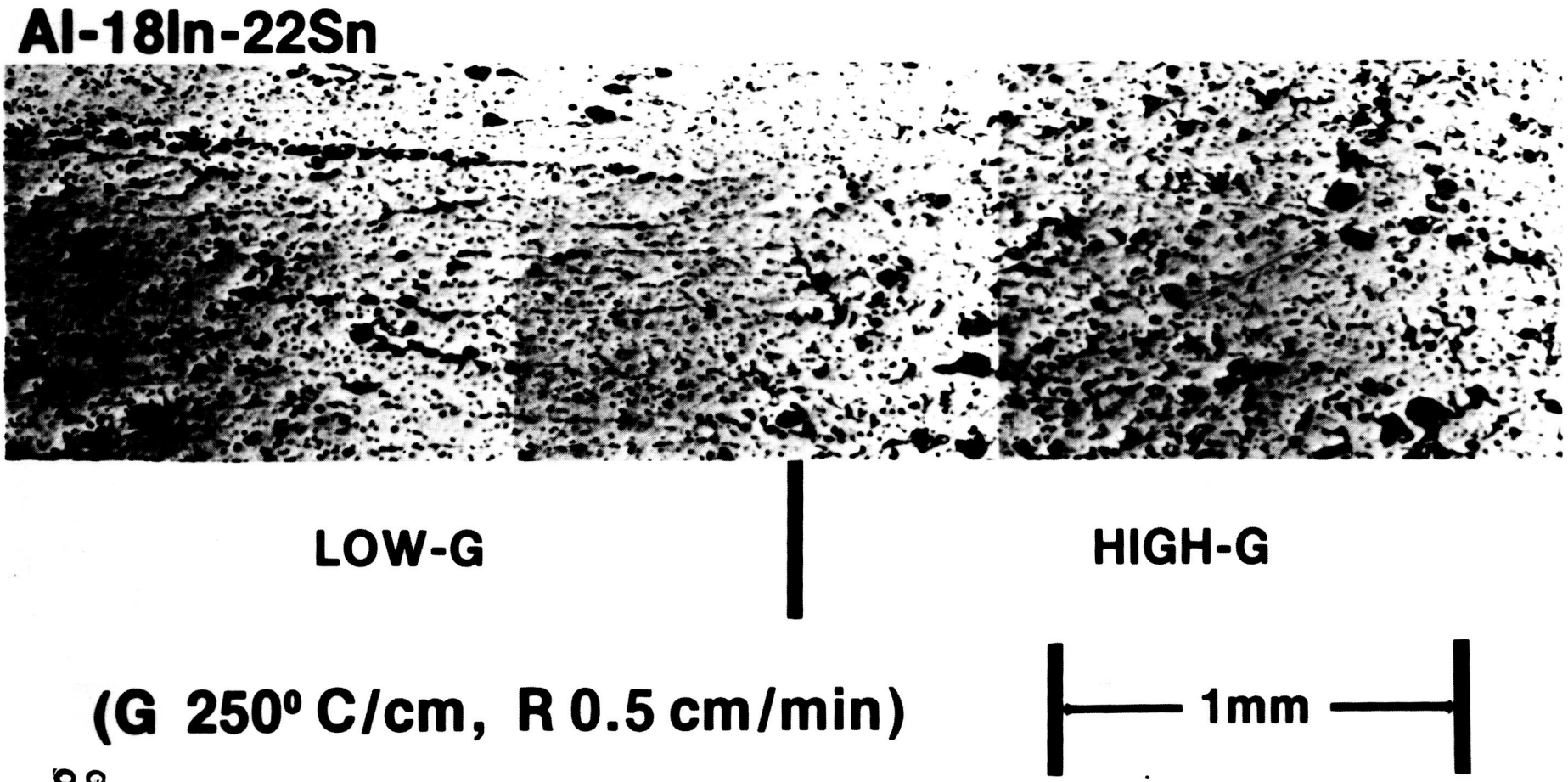

Figure 17. Microstructural transition between low and high gravity during the fourth parabolic maneuver for Al-18.1In-22Sn.

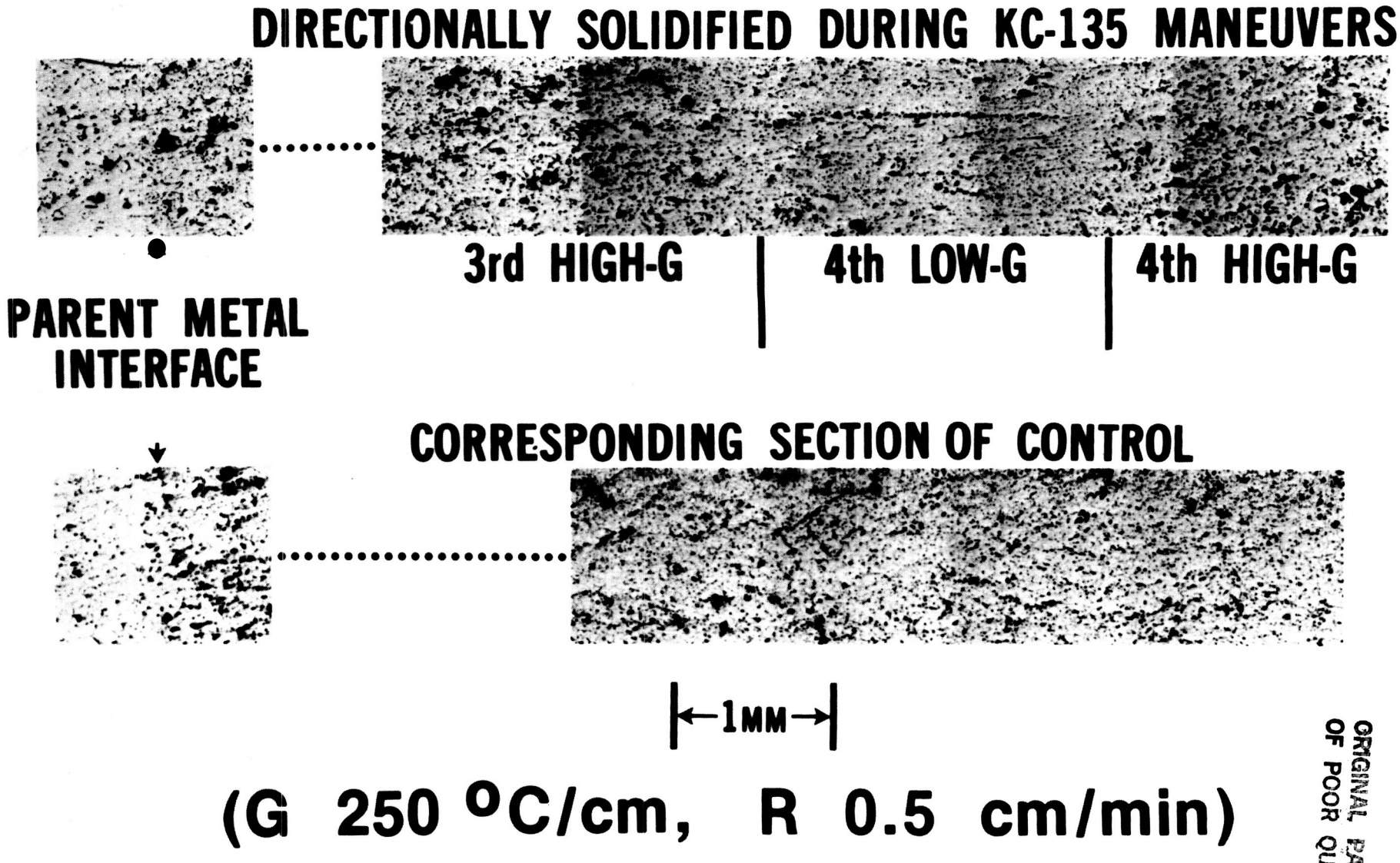

Figure 18. Microstructure around the fourth low-gravity zone relative to a corresponding section of the control sample for Al-18.1In-22Sn.

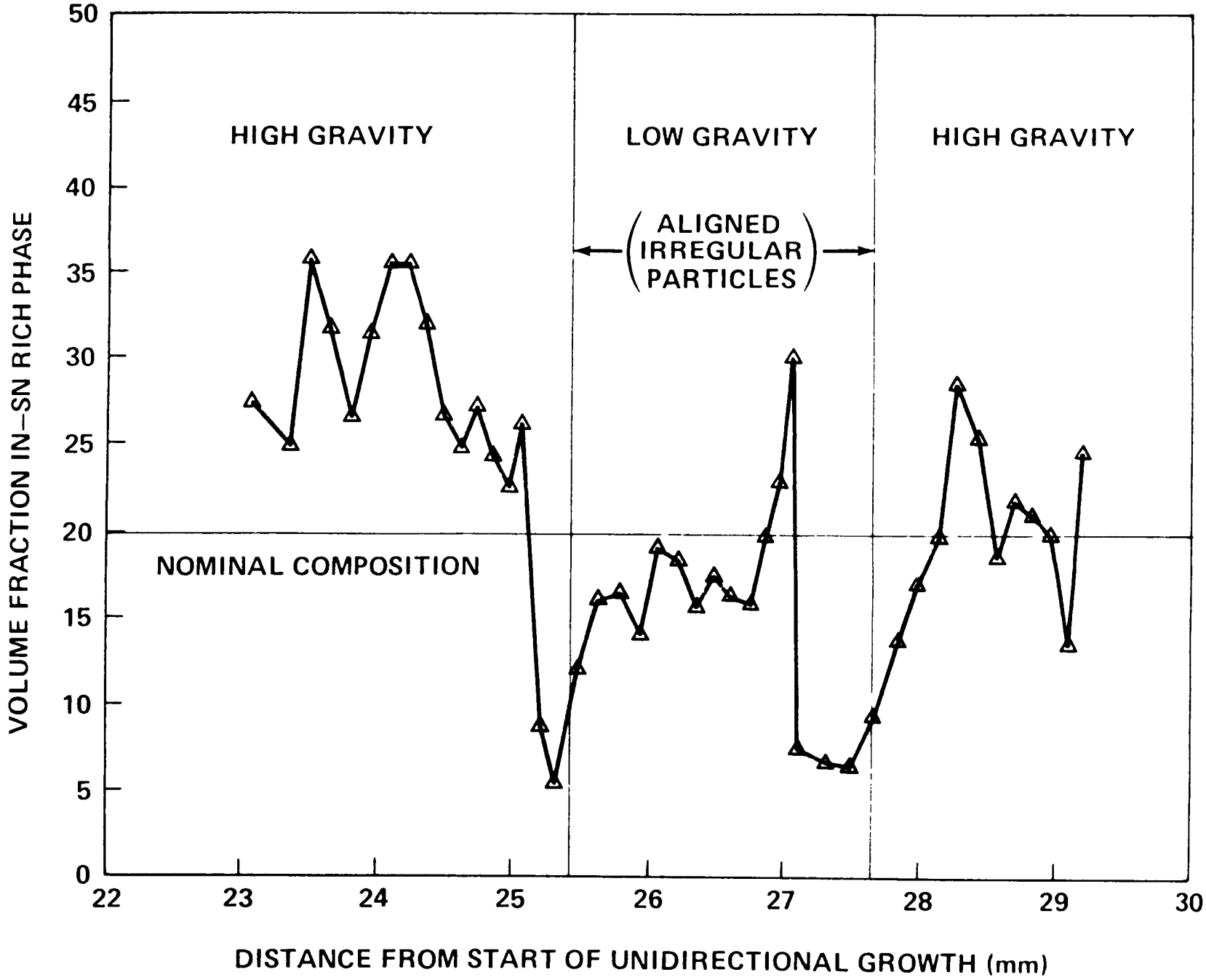

Figure 19. Quantitative microscopy for Al-18.1In-22Sn flight sample around the fourth low-gravity zone.

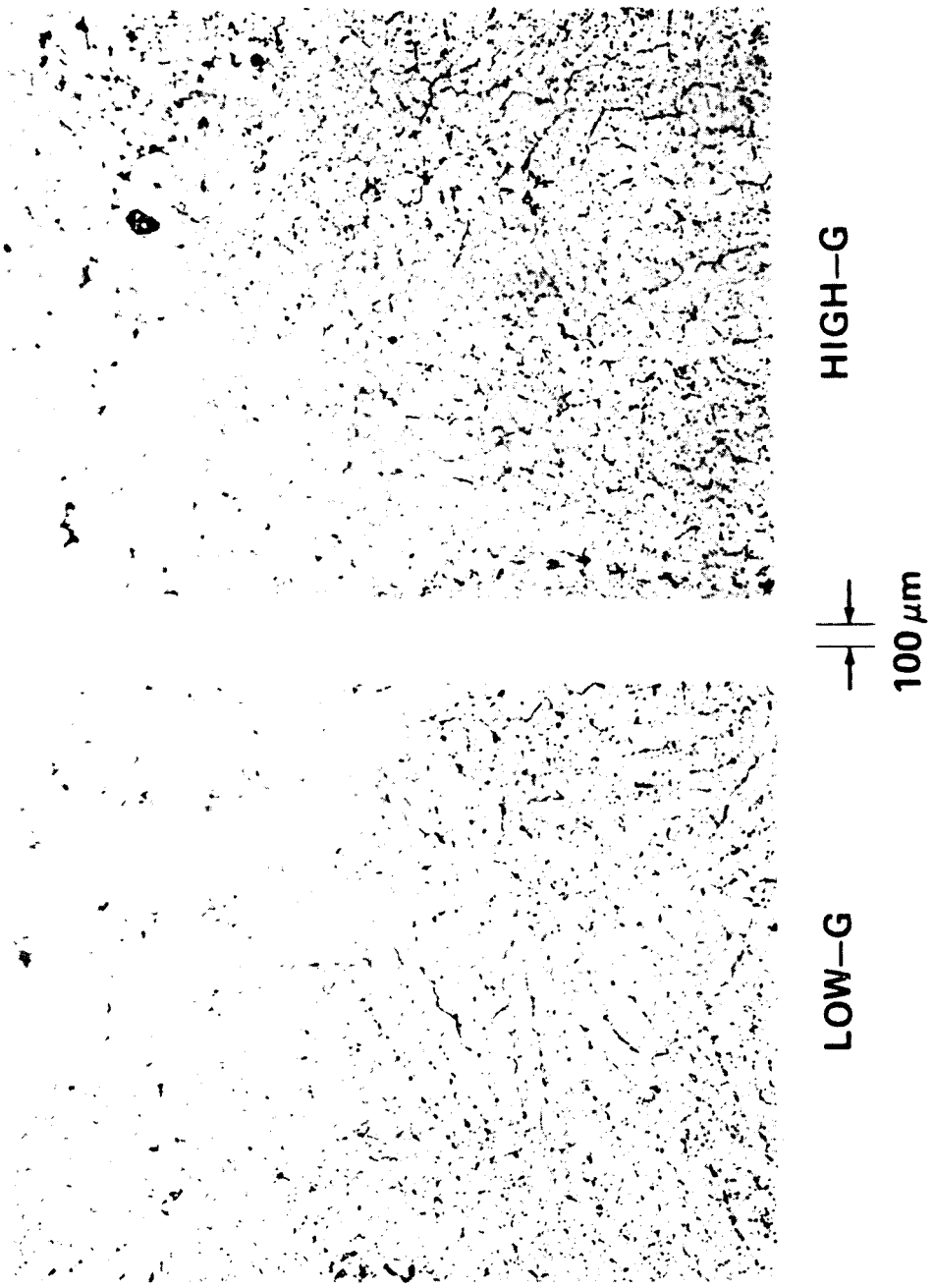

Figure 20. Transverse sections for Al-18.1In-22Sn flight sample through the fourth low-and high-gravity zones.

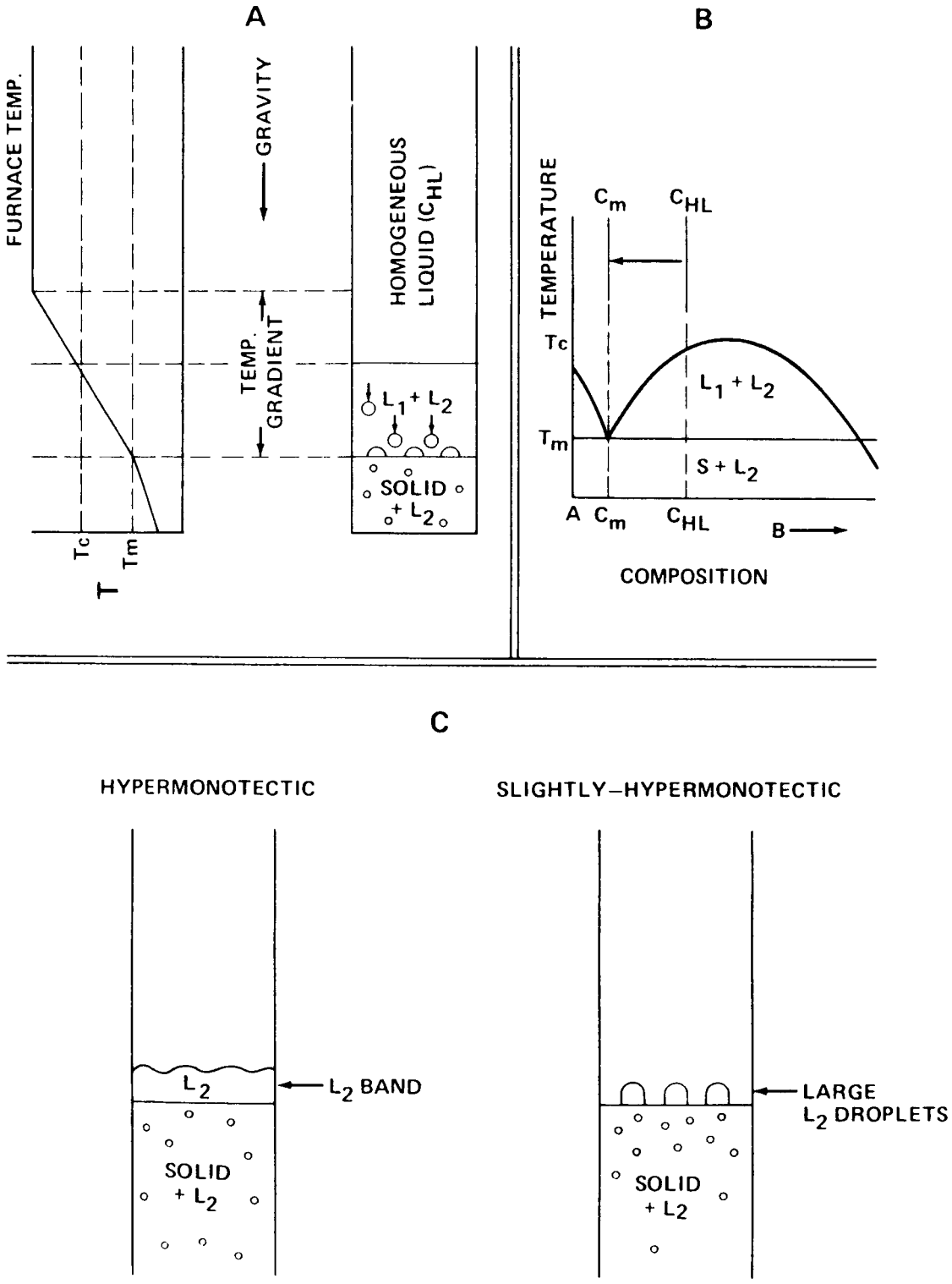

Figure 21. Liquid composition gradient resulting from a hypermonotectic sample under gravity in a temperature gradient. (A) Temperature gradient and resulting separation (density of L_2 is greater than L_1). (B) Resulting change in composition of the homogeneous liquid. (C) Resulting liquid composition profile for hypermonotectic and slightly hypermonotectic starting compositions.

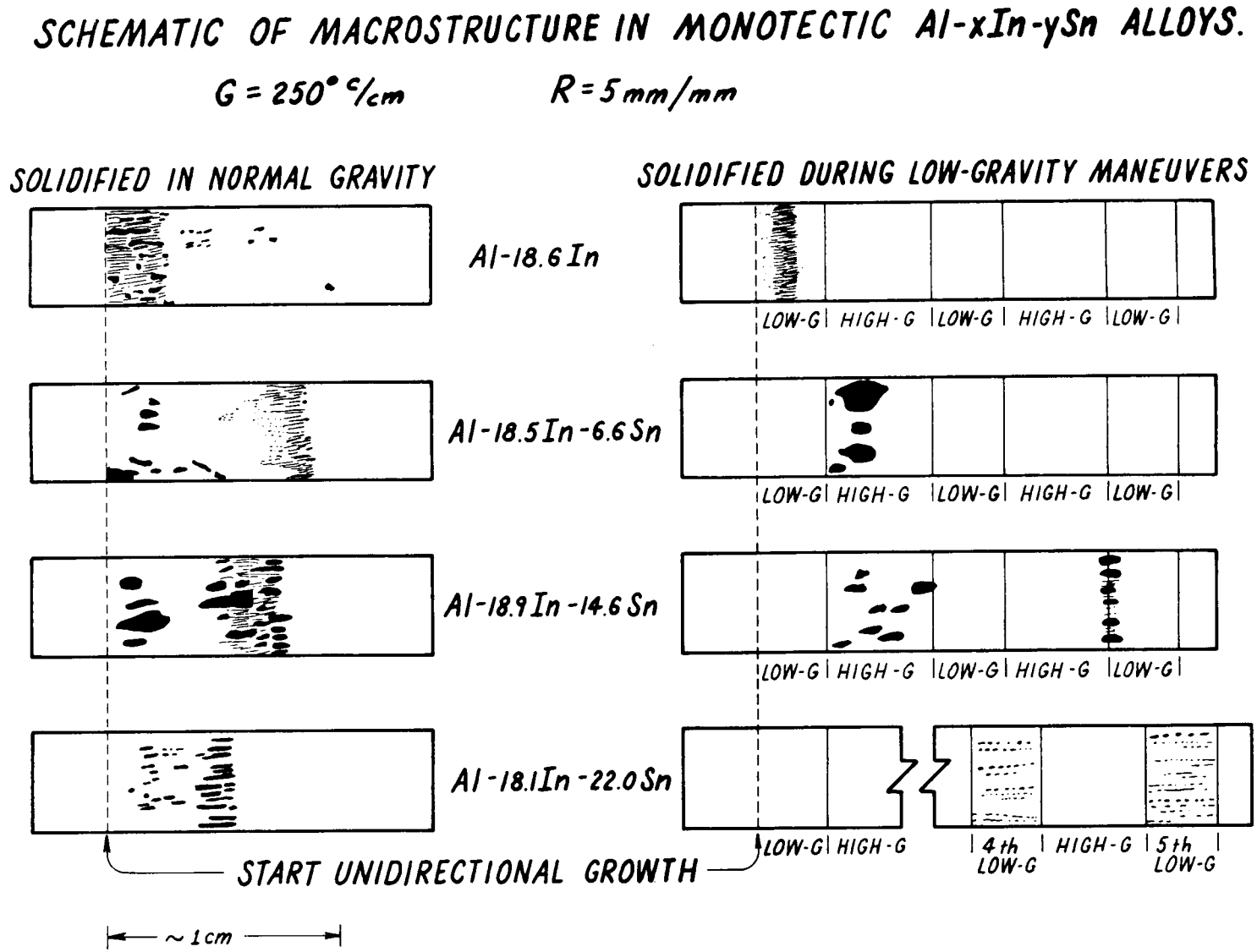

Figure 22. Schematic summary of the macrostructures of Al-x.In-y.Sn hypermonotectic alloys directionally solidified upwards in one gravity and directionally solidified during KC-135 low-gravity maneuvers.

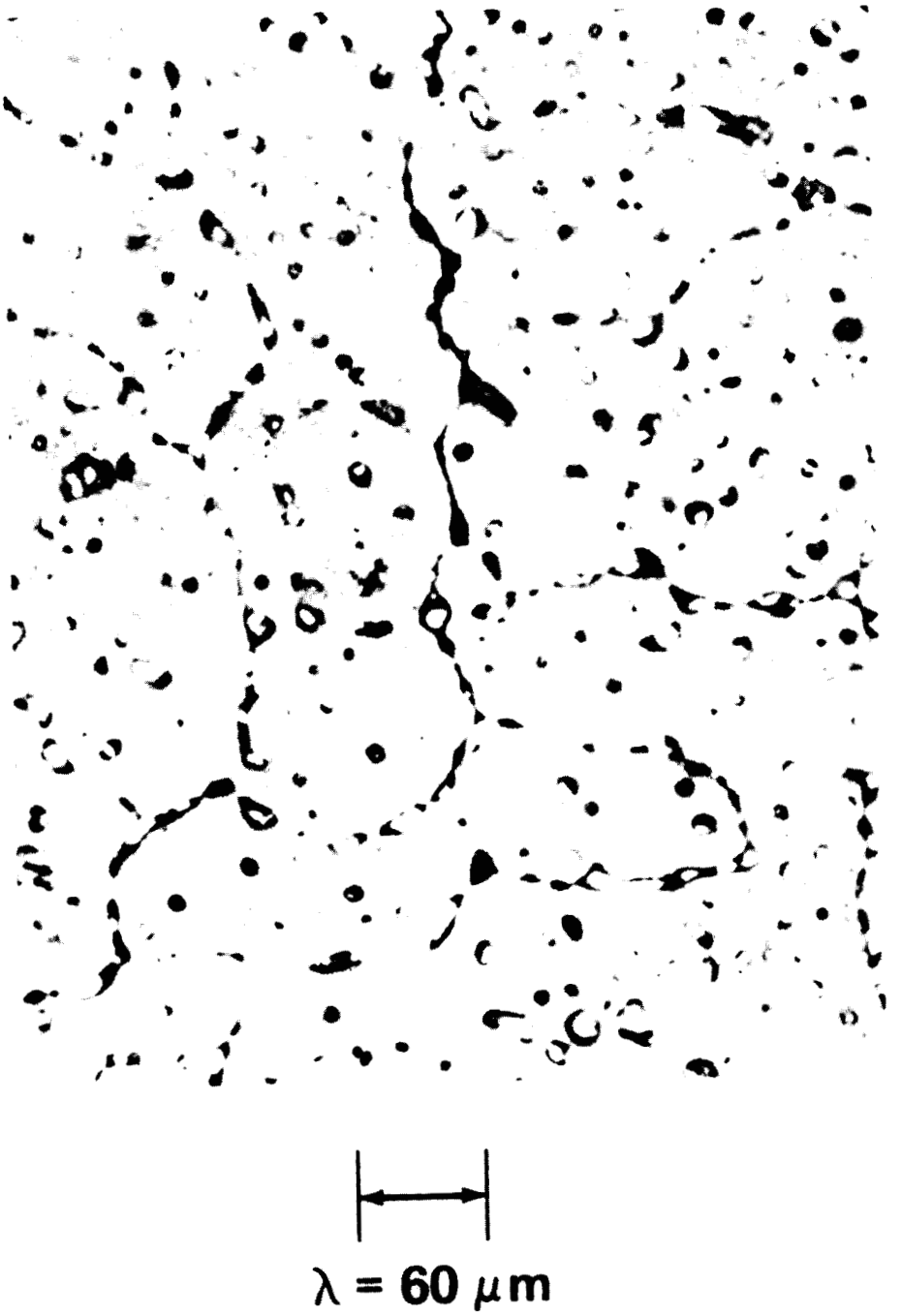

Figure 23. Transverse section through the fourth low-gravity zone for Al-18.1In-22Sn flight sample showing the relative size of the spacing of the aligned particles.

APPROVAL

THE EFFECTS OF GRAVITY LEVEL DURING DIRECTIONAL SOLIDIFICATION ON THE MICROSTRUCTURE OF HYPERMONOTECTIC Al-In-Sn ALLOYS

Center Director's Discretionary Fund Final Report

By P. A. Curreri and W. F. Kaukler

The information in this report has been reviewed for technical content. Review of any information concerning Department of Defense or nuclear energy activities or programs has been made by the MSFC Security Classification Officer. This report, in its entirety, has been determined to be unclassified.

E. A. Tandberg-Hanssen

E. A. TANDBERG-HANSSEN
Deputy Director, Space Science Laboratory

☆U.S. GOVERNMENT PRINTING OFFICE 1987 730-067/40050